


Cite this: *RSC Adv.*, 2025, **15**, 6875

## Metal oxides and their composites for the remediation of organic pesticides: advanced photocatalytic and adsorptive solutions

Ayman H. Kamel, <sup>\*ab</sup> Hisham S. M. Abd-Rabboh, <sup>c</sup> Ahmed Abd El-Fattah, <sup>ad</sup> Ghizlane Boudghene Stambouli<sup>ae</sup> and Lina Adeida<sup>ae</sup>

Metal oxide nanoparticles and their composites have garnered significant attention in water treatment and environmental cleanup due to their unique physicochemical properties. These materials exhibit distinct crystalline structures, tunable morphologies, large surface areas, versatile surface chemistry, and widespread availability. These features make nanostructured metal oxides and their composites highly effective for the selective removal of organic pollutants from the environment, either by adsorption or photodegradation. This article focuses on recent advances, challenges, and opportunities in the use of metal oxides and their composites for the targeted removal of organic contaminants, including insecticides, phenolic compounds, organic dyes, and similar pollutants. The discussion encompasses a broad range of metal oxides and their composites, highlighting their diverse structural, crystallographic, and morphological characteristics that influence their adsorption and photocatalytic performance. Emphasis is placed on the photocatalytic and adsorptive capabilities of these materials, including their photo-stimulation properties and mechanisms. Metal oxides are highlighted as outstanding photocatalysts due to their high photodegradation efficiency, cost-effective synthesis methods, and optimized bandgap engineering. This review serves as a valuable resource for researchers exploring the photocatalytic and adsorptive applications of metal oxide-based materials, particularly in the remediation of hazardous organic pollutants such as pesticides.

Received 16th November 2024

Accepted 22nd December 2024

DOI: 10.1039/d4ra08149h

[rsc.li/rsc-advances](http://rsc.li/rsc-advances)

<sup>a</sup>Department of Chemistry, College of Science, University of Bahrain, Zallaq P. O. Box 32038, Bahrain. E-mail: ahmohamed@uob.edu.bh

<sup>b</sup>Department of Chemistry, Faculty of Science, Ain Shams University, Cairo 11566, Egypt. E-mail: ahkamel76@sci.asu.edu.eg

<sup>c</sup>Chemistry Department, Faculty of Science, King Khalid University, Abha 61413, Saudi Arabia

<sup>d</sup>Department of Materials Science, Institute of Graduate Studies and Research, Alexandria University, Alexandria 21526, Egypt

<sup>e</sup>Department of Chemistry, Inorganic Chemistry and Environment Laboratory, University of Tlemcen, P. O. Box 119, 13000 Tlemcen, Algeria



Ayman H. Kamel

Prof. Kamel has completed his PhD degree from Ain Shams University, Cairo, Egypt with a focus on the fabrication and characterization of electrochemical sensors for environmental, biomedical and pharmaceutical analysis. Prof. Kamel has published over 137 research articles in well reputed high impact factor international journals. He is also the author of several book chapters. He serves as guest editor, member, referee, and reviewer for many international renowned scientific journals. He has successfully completed several research projects as Principal Investigator. Professor Ayman H. Kamel is a leading figure in the field of sensors and their applications. His research primarily focuses on developing novel sensor technologies and exploring their potential applications in various fields such as healthcare, environmental monitoring, and industrial automation. Prof. Kamel has made significant contributions to the development of sensors with improved sensitivity, selectivity, and reliability. His work often involves interdisciplinary collaboration, combining principles from fields such as materials science, electrical engineering, and chemistry to advance sensor technology. One of his notable achievements is in the area of biomedical sensors, where he has worked on developing sensors for early disease detection, monitoring of physiological parameters, and drug delivery systems. These sensors have the potential to revolutionize healthcare by providing real-time monitoring and personalized treatment options.



## 1. Introduction

Wastewater contains a variety of substances, including those that are organic (such as pathogens), inorganic (such as heavy metal ions, metal oxides, metal complexes, salts, and other inorganic substances), and nutrient- and agricultural-runoff-related. Organic pollutants are attracting a lot of interest due to their (a) varied applications and subsequent discharge to terrestrial and aquatic bodies; (b) prolonged persistence; (c) high resistance to degradation; and (d) considerable health and environmental consequences.<sup>1</sup> About 85–90% of all fresh water is used for irrigation of agricultural land in Africa and Asia.<sup>2</sup> Agriculture continues to be the predominant user of global freshwater resources, representing approximately 70% of total withdrawals, with variations observed across regions due to differing irrigation practices.<sup>3</sup> The issue of pesticide contamination remains a critical challenge, as residues from agricultural runoff continue to impact major rivers and aquatic ecosystems worldwide.<sup>4</sup> The two issues underscore the critical necessity for sustainable water management practices within the agricultural sector.<sup>5</sup>

Pesticides are the main cause of organic pollutants in water bodies. Pesticides primarily enter the aquatic system from (a) personal usage, (b) pesticide production industry effluents, and (c) the agriculture sector, where they are heavily used for pest management to protect crops from pest damage. Insecticides, herbicides, fungicides, rodenticides, and plant growth regulators are examples of pesticides. Uncontrolled and excessive pesticide usage contaminates water (agricultural runoff) and is harmful to aquatic life and human health. The current WHO guidelines for drinking water quality specify that acceptable levels of pesticides depend on individual compounds.<sup>6</sup> For instance, guideline values are derived based on toxicity and potential exposure. The maximum acceptable values for individual pesticides often fall within  $0.1 \mu\text{g L}^{-1}$  to  $1 \mu\text{g L}^{-1}$  for specific compounds, with stricter limits for more hazardous pesticides. For total pesticides, the cumulative limit generally aligns with  $0.5 \mu\text{g L}^{-1}$ , but this varies depending on local regulations and risk assessments.<sup>6</sup> Pesticides that are used in excess of the allowed amount can have harmful effects on human health, including endocrine, gastrointestinal, neurological, respiratory, reproductive, and dermatological issues.<sup>7</sup> Contaminated water contributes to scarcity because it becomes unusable for domestic, agricultural, or industrial purposes, reducing the overall accessible water supply. This exacerbates water scarcity, especially in regions where clean water resources are already limited. Water demand has increased because of rising population, economic development, urbanization, dynamic changes in lifestyle, attitudes about water use, and rapid industrialization.<sup>8</sup> Water scarcity is a danger in many parts of the world, and many people are unable to meet their basic needs. As a result, much effort has been made to conserve water and remove toxins from wastewater so that it can be used for domestic and agricultural purposes. The removal of various types of organic pollutants from wastewater using cost-effective and ecologically friendly approaches is a hot topic. The study of

the interaction between organic contaminants in water and the materials that may be used to remove or degrade them quickly and cheaply is becoming increasingly important for technological application in this context.

The transition metal oxide nanoparticles are appealing candidates for the adsorption process because of their exceptional surface properties, microstructural features, and large surface area.<sup>9</sup> The increased surface area and active sites make adsorption events simpler. Nanoscale properties, such as high surface-to-volume ratios and increased active sites, enhance adsorption kinetics by providing more interaction points for pollutant molecules. Thermodynamically, the high surface energy at the nanoscale facilitates stronger binding interactions, leading to favorable adsorption equilibria. In order to remove organic contaminants from wastewater, nanoparticles have superior adsorption capability than their bulkier cousins. Metal oxide nanoparticles, either alone or in combination, have demonstrated tremendous promise recently as highly selective adsorbents for the quick and effective removal of organic contaminants from wastewater.<sup>10</sup>

## 2. Pesticide: risks and benefits

Pesticides are lethal chemical or biological substances that are released into the environment to reduce, eliminate, or control the population of insects, weeds, rodents, fungi, and other pests.<sup>11</sup> The main sources of pesticides in the environment are forestry and agriculture. Even though it is well known that a growing world population needs greater global food production, it is desirable for the pesticide to kill the target organisms to reduce the impact of weed species on both humans and the environment. On the other hand, these organic pollutants could destroy the ecosystem's flora and wildlife if they are applied improperly. In addition, humans and other living things are more negatively impacted by the widespread use of these dangerous chemical pesticides.

Hazardous pesticides are widely used against various organisms. Among them, 80% of pesticide applications are targeted at insect control, followed by 15% for herbicide use and 1% for treating plant fungal diseases, with the remaining 4% used for other purposes. When categorizing the types of pesticides by frequency of use, insecticides constitute 47.5%, herbicides 29.5%, fungicides 17.5%, and other chemicals 5.5%. This discrepancy likely arises from differences in classification—one based on the purpose of application and the other on the types of pesticides sold or applied.<sup>12</sup> The long-term consequences of pesticides and the influence of hazardous chemicals released into water bodies are well known to environmental specialists and farmers.<sup>13</sup> In the past 50–60 years, there has been a rise in the incidence of cancer and chronic diseases because chemical pesticides act as catalysts for carcinogens.<sup>14</sup>

Hazardous chemical pollutants accumulated in the soil have been reduced using treatment techniques like leaching and landfilling. On the other side, the soil remediation process takes a long time and is expensive. To safeguard farmland and limit the use of harmful pesticides, organic waste/earthworm techniques and manure as a soil amendment are required.



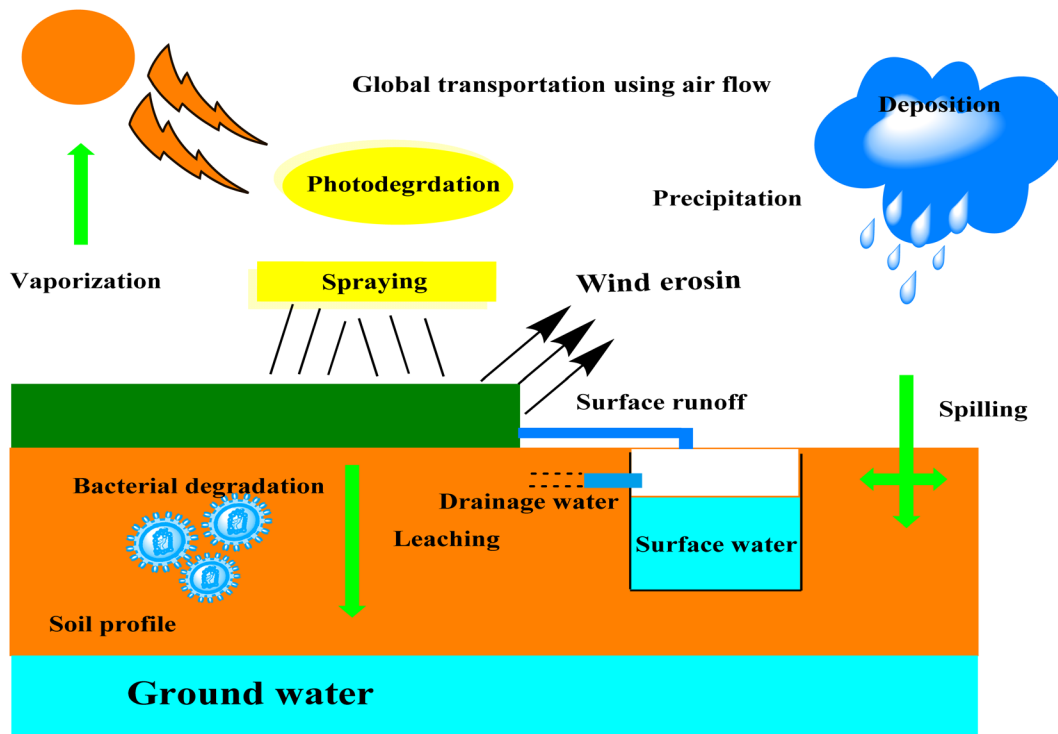


Fig. 1 Different stages of pesticide cycle that reach the ground and surface water.

Numerous beneficial bacteria can create surfactants.<sup>15</sup> On the other hand, more research approaches are needed to address environmental and procedural problems that need in-depth examination to broaden their scope. In recent years, bioremediation techniques, such as the use of microorganisms and metabolic enzymes to break down pesticides and change them into another form through sludge formation, have become less toxic.<sup>16</sup> But many defaulters nevertheless restrict their regular use in a hazardous environment and environmental restoration.<sup>17</sup>

Due to the existence of pesticide toxins and their impact on water quality and agricultural soils through their use, which may be damaging to all forms of life, the problem of pollution is a cause of concern for many developing and developed countries. Although a larger dose of a pesticide can injure humans more than the intended pest, humans can be killed in a variety of ways with very tiny quantities.<sup>18</sup>

Inhibiting sex hormones, impairing ovarian function, and damaging endocrine glands are all fatal impacts of pesticides.<sup>19</sup> Due to their heightened biological function and quick toxicity, pesticides are categorized as being extremely damaging, highly poisonous, and moderately dangerous. The compounds dimethoate, quinalphos, and dichloro-diphenyl-trichloroethane are all a little dangerous. Malathion is a very dangerous substance. Atrazine and other carbamates are unlikely to present a serious concern.<sup>20</sup> If toxic pesticides are misused, agricultural producers are particularly vulnerable to their negative effects.<sup>21</sup> Pesticides tend to settle as sediments, which can turn agricultural soils into a source of organochloride pollutants that can spread and volatilize and pose a risk to the surfaces of soil and water (Fig. 1).<sup>22</sup>

Pesticides can kill and injure soil-dwelling microorganisms, particularly when these substances are employed improperly or excessively, which causes chemical compounds to accumulate in the soil.<sup>23</sup> These chemicals may take several years to break down. Incomplete knowledge exists regarding how pesticides affect soil microorganisms. Numerous studies have shown that pesticides harm soil microorganisms and biochemical processes, whereas other studies have shown that microorganisms break down and absorb pesticide residues.<sup>24</sup>

Pesticides have different impacts on different types of soil microorganisms depending on their stability, concentration, and toxicity, as well as several environmental factors.<sup>24</sup> It is challenging to make definitive judgements about the relationship between pesticides and soil ecology due to the intricate interactions between the variables. The overall metabolic systems governing the nutrition cycle may become compromised by prolonged pesticide use.<sup>24</sup> Additionally, herbicides like triclopyr affect the soil's ability to convert ammonia to nitrite.<sup>25</sup> The ability to measure changes in the various settings of pesticide-treated soil would be greatly enhanced by improved operational allocations of bacterial taxonomic groups.<sup>25</sup> Water serves as a binder, making it simple for pesticides to penetrate moist soil.<sup>26</sup> The amount of pesticide that affects the soil varies according to soil humidity, temperature, sunshine, plants, and physiological features of the soil.<sup>9</sup>

### 3. Pesticides classifications

Based on their composition, level of toxicity, and intended use, pesticides are classified. The most common technique for classifying pesticides is based on the chemical properties of the



Table 1 Classification of organic pesticides based on their origin<sup>2,9,10</sup>

Origin	Source	Class	Example	Feature
Organic	Natural	Plants phytochemical	Essential oil, plant extracts, and leftover oilseed cakes	Low toxicity, limited persistent in environment, and complicated structures that prevent resistance in pests
	Synthetic	Pyrethroids	Phenthion, diazinon, cypermethrin, deltamethrin, cyfluthrin, and cypermethrin	Effect the sodium channel in insects resulting in paralysis of the organism, highly toxic to insects and fish but less to mammals, unstable upon the exposure of light, and commonly used in food
		Organophosphates	Aldrin, dieldrin, glyphosate, and chlorpyrifos	Cause paralysis resulting in death, and dominant for variety of pests
		Carbamates	Deltamethrin, cypermethrin, fenvalerate, permethrin, cyfluthrin, cyhalothrin, cypermethrin, and carbofuran	Effect the nerve of the pests resulting in poisoning and death, and low pollution caused upon degradation
		Organochlorine	Chlorothalonil and endrin aldehyde	Used for insects, long persistent in environment, and affect the nerve system causing paralysis and death of the pests

pesticide (Table 1) and the characteristics of the target (Table 2). Based on their chemical makeup, pesticides are classified as organochlorines, organophosphorus, carbamates, pyrethrins, and pyrethroids (Table 3). Most insecticides used nowadays are organic and include both synthetic and plant-specific pesticides.<sup>27</sup> Based on the structure, toxicity, and functional categories of pesticides; more groupings are created. Pesticides are used in several ways to prevent the spread of pests or manage their numbers. Some herbicides are used to prevent plant growth, while others have effective photosynthetic control.<sup>28</sup> Nearly all insecticides have the potential to significantly impact the ecosystem. They pose a serious risk to the ecosystem.<sup>28</sup> Fungi and their spores are killed or have their growth slowed by substances referred to as fungicides.<sup>29</sup> Fungicide misuse, storage, and release into moving water all present significant contamination risks.<sup>30</sup>

#### 4. Overview of water cleanup methods

Organic dyes, insecticides, medicines, fertilizers, surfactants, and other chemicals can be found in a wide variety of products. Conversely, excessive use, environmental discharge or disposal, and inadequate treatment contaminate water sources and have detrimental effects on our ecosystem, including humans. As a result, it has proven difficult to eliminate organic pollutants from wastewater. There were numerous efforts made to eliminate or degrade organic pollutants from the water. Utilizing a range of physical, chemical, and biological methods, organic pollutants, and the breakdown products they produce are eliminated or reduced from the aquatic environment (Fig. 2). These techniques are used individually or in combination with others to detoxify contaminated wastewater. Adsorption, membrane filtration, biological degradation, photocatalytic degradation, nanofiltrations, oxidation, reverse osmosis, UV radiation, and other techniques are used to disinfect water.<sup>31,32</sup> The greatest techniques for eliminating pesticides, beta

blockers, and medications have been discovered to be chemical oxidation processes such as ozonation ( $O_3$ ), UV photolysis, and photo-Fenton processes.<sup>33</sup> Among other biological processes, membrane filtration remediation (MFR), activated sludge, and aeration methods were superior at removing endocrine distributing chemicals (EDCs) [*i.e.* endocrine-disrupting chemicals (EDCs) are compounds that interfere with the hormonal systems of organisms, potentially causing adverse developmental, reproductive, neurological, and immune effects].<sup>34</sup> With the activated sludge technique, surfactants, EDCs, and personal care products (PCPs) can be effectively eliminated.<sup>35</sup> Reviewing the importance of employing metal oxide nanocomposites in water remediation is the main goal of this article. The field of wastewater photocatalysis using photocatalyst nanocomposite is driven by ultraviolet (UV) and visible light. Using different kinds of organic waste, full studies showed that photocatalysis led to complete and efficient degradation and the creation of less harmful, eco-friendly products.<sup>36</sup> Toxic byproducts, however, may have been produced because of partial breakdown.<sup>36</sup> Adsorption and photocatalysis are economically scalable due to their reliance on abundant and inexpensive materials (*e.g.*, activated carbon, metal oxides). For instance, the use of sunlight in photocatalysis reduces energy costs, while adsorption processes benefit from renewable or waste-derived adsorbents like biochar.

Recent studies have highlighted the effectiveness of metal oxide nanostructures, particularly  $TiO_2$ -ZnO composites, in treating water contaminated with persistent organic pollutants.<sup>37</sup> Exposed to visible light, these nanostructures show significantly higher degradation rates than conventional methods, a critical advancement that could favor their use under ambient light conditions.<sup>37</sup> This research demonstrates how optimizing the structure and porosity of composites can accelerate degradation processes, reducing energy demands and enhancing water purification efficiency under natural conditions.<sup>38</sup>



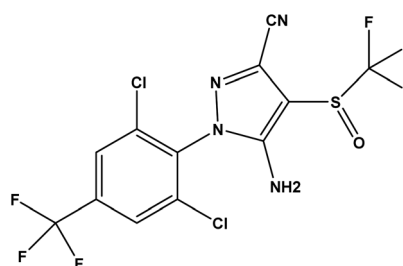
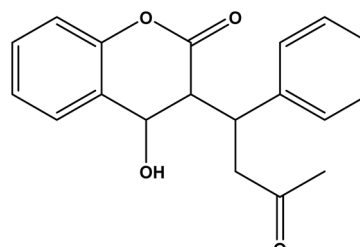
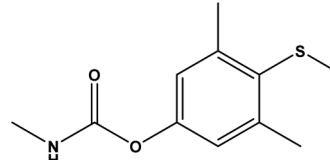
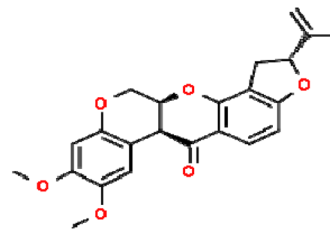
Table 2 Classification of pesticides based on target<sup>3,5,11</sup>

Class	Example	Target pests	
Acaricides	Bifonazole	Mites	
Avicides	Avitrol (4-amino pyridine)	Birds	
Fungicides	Azoxystrobin	Fungi	
Herbicides	Atrazine	Weeds	
Insecticides	Aldicarb	Insects	
Larvicides	Methoprene	Larvae	
Molluscicides	Metaldehyde	Snail	
Nematicides	Aldicarb	Nematodes	
Ovicides	Benzoxazine	Egg – prevents hatching of egg in insects and mites	



Table 2 (Contd.)

Class	Example	Target pests
Piscicides	Rotenone	Fishes
Repellents	Methiocarb	Insects
Rodenticides	Warfarin	Rodents
Termiticides	Fipronil	Kills termites



## 5. Metal oxides-based nanostructured materials

Metal oxide nanoparticles have been studied in a variety of applications, including energy storage, catalysis, electrochemistry, lubrication, sensors, coatings, environmental remediation, and others.<sup>39,40</sup> The surface properties, microstructural features, and high surface area of transition metal oxide nanoparticles make them suitable candidates for the adsorption process.<sup>41</sup> Adsorption is aided by the active sites and large surface area. When the size of materials is lowered from bulk to nano, the surface-to-volume ratio increases rapidly.<sup>42</sup> When it comes to removing organic pollutants from wastewater, nanoparticles have a better adsorption capability than their bulkier counterparts. Activated carbon derived from biomass, as well as novel forms of carbon such as graphene, carbon nanotubes, fibers, and others, displayed good organic pollutant adsorption capabilities in wastewater.<sup>43</sup> Metal oxide nanoparticles have

lately shown significant promise as highly selective adsorbents for the quick and effective removal of organic pollutants from wastewater,<sup>44</sup> either as single materials or as composites. Transition metal oxides and their composites have excellent photocatalytic activity for destroying organic pollutants.<sup>45</sup> Wide band gap semiconductors with non-toxicity and water stability for photocatalytic oxidation/degradation of organic pollutants are made from metal oxide-based nanomaterials with well-controlled structural, crystalline, and surface characteristics. Recent advancements in metal oxide nanostructures research have significantly boosted their adsorption and photocatalytic capabilities. For instance, a 2023 study demonstrated that TiO<sub>2</sub> and ZnO nanoparticles, modified with rare-earth dopants, offer increased active sites, allowing for more intensive interactions with pollutants and thereby enhancing degradation efficiency in diverse settings.<sup>46</sup> Adjusting morphology and composition makes these metal oxides particularly promising for use under various environmental conditions.<sup>1</sup>



**Table 3** Classification of pesticides based on their chemical makeup<sup>14–16</sup>

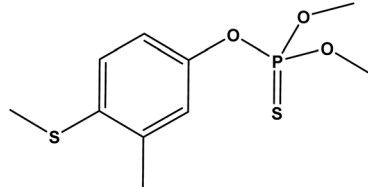
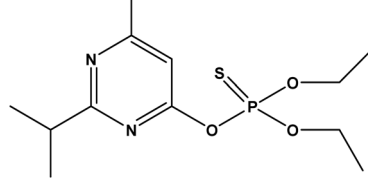
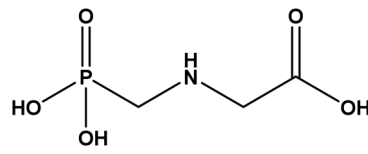
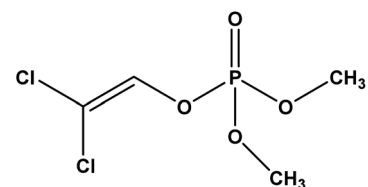
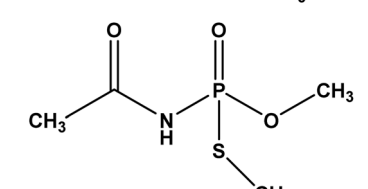
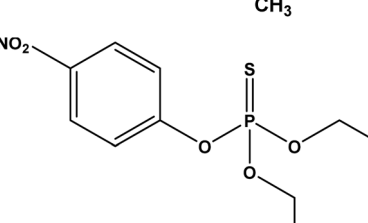
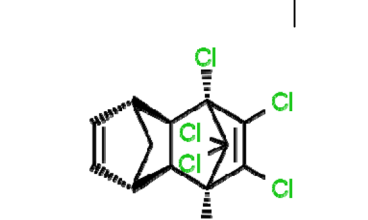
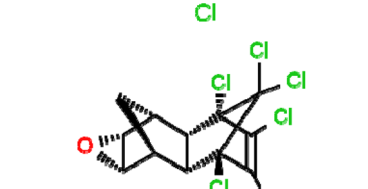
Category	Name	Chemical structure
	Phenthion	
	Diazinon	
	Glyphosate	
Organophosphorous	Dichlorvos	
	Acephate	
	Parathion	
Organochlorine	Aldrin	
	Dieldrin	
	Cypermethrin	

Table 3 (Contd.)

Category	Name	Chemical structure
	Chlorpyrifos	
	Cyfluthrin	
	Chlorothalonil	
	Endrin	
	Carbaryl	
Carbamates		
	Carbofuran	
	Methomyl	



Table 3 (Contd.)

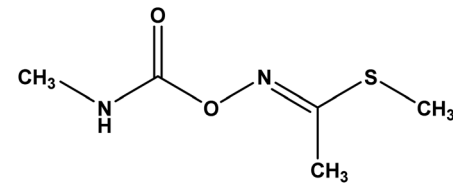
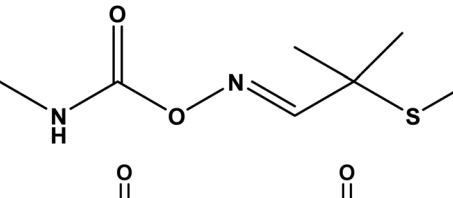
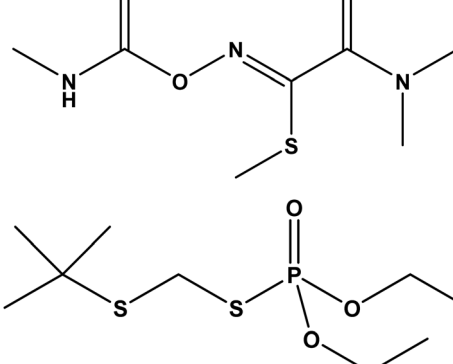
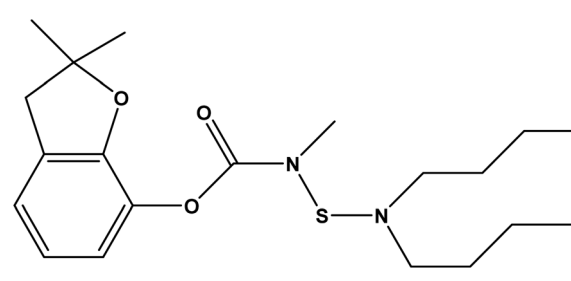
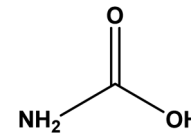
Category	Name	Chemical structure
		
	Aldicarb	
	Oxamyl	
	Terbufos	
	Carbosulfan	
	Carbamic acid	

Photo-degradation has long been seen to be one of the most environmentally friendly ways to remove organic pollutants from water.<sup>47</sup> It has several advantages, including the use of renewable energy (solar energy) and the conversion of organic contaminants into non-toxic molecules and gases.<sup>48</sup> Metal oxide semiconductors only use a small fraction of the solar spectrum, specifically UV light (5% of the solar spectrum),<sup>49</sup> which is a major limitation of the photocatalytic process. This disadvantage can be solved through band gap engineering of metal oxide nanoparticles, which comprises chemical and structural changes, heteroatom doping, and nanocomposites.

The best photocatalysts absorb the visible spectrum efficiently, delay hole and electron pair recombination, and perform well as photocatalysts.<sup>50</sup> Metal oxide nanoparticles, such as iron oxides,  $\text{Al}_2\text{O}_3$ ,  $\text{TiO}_2$ ,  $\text{CuO}$ ,  $\text{ZnO}$ ,  $\text{CeO}_2$ , and others, have attracted interest as adsorbents and photocatalysts.<sup>51,52</sup> For enhancing performance efficiency and selectivity, porous materials-supported metal oxides, magnetic metal oxides, metal–metal oxides, graphene–metal oxides, and other metal oxide-based nanocomposites have all been explored.<sup>53,54</sup> The size, texture, and surface characteristics of these nanomaterials influence the adsorption events.<sup>37,39,41,44</sup> Various morphologies



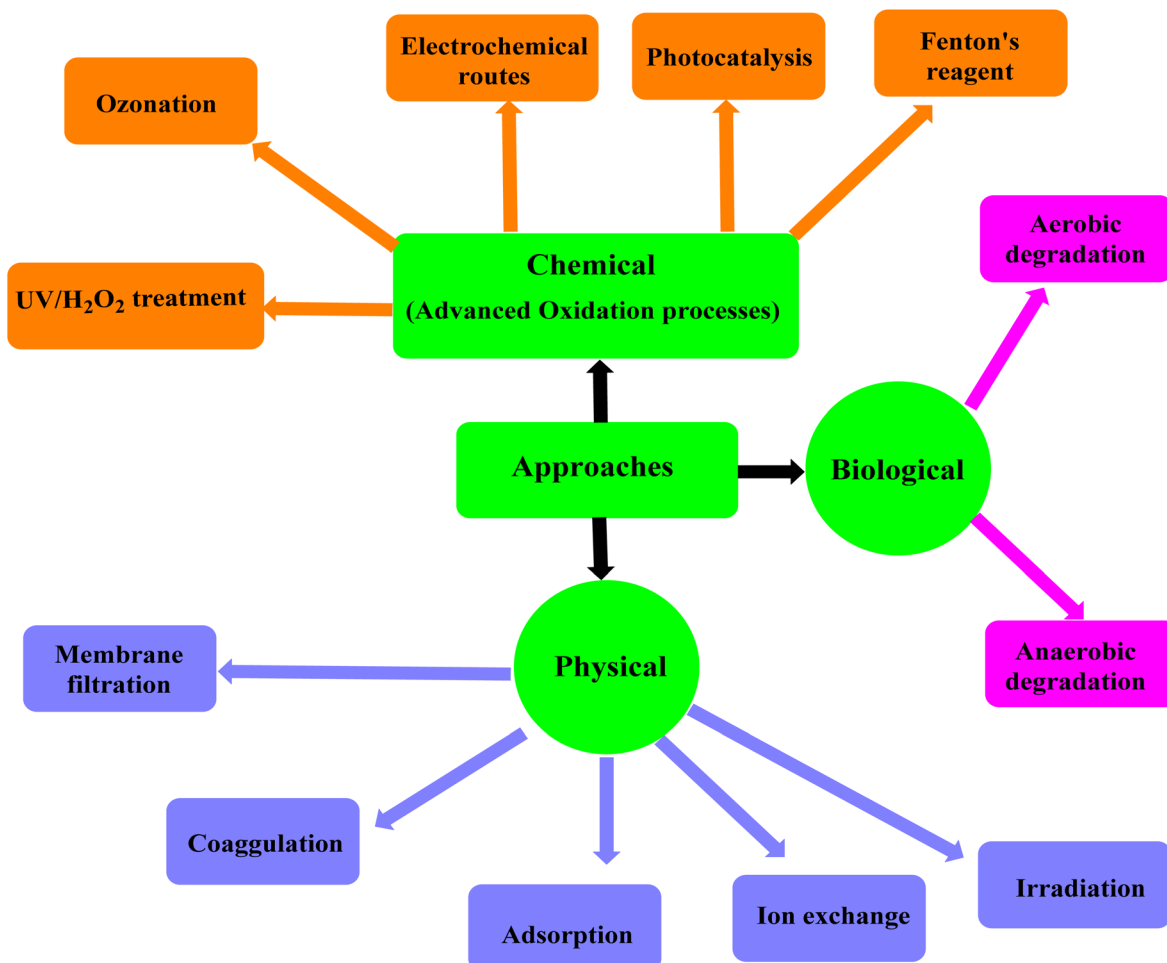


Fig. 2 Chemical, biological, and physical approaches to remove or degrade the organic pollutants in the wastewater.

of nanoparticles provide distinct crystal facets as active sites on the surface of materials for adsorption and photocatalytic applications. Bhatti *et al.*<sup>55</sup> examined the effect of ZnO nanoparticle shape on the photocatalytic degradation of methyl orange dye. This research examines the structural, crystalline, and surface properties of a variety of metal oxide nanoparticles and their nanocomposites for wastewater treatment *via* adsorption and photocatalytic destruction of organic pollutants.

Metal oxide nanostructures have been shown to be effective and flexible in cleaning up the environment, which shows how useful they could be. However, it is also important to think about how safe they are for the environment and how easily they can be recycled for long-term use. Metal oxide nanoparticles, when released into the environment, may present significant risks to aquatic organisms and soil ecosystems because of their elevated reactivity and durability. To address these risks, approaches like surface functionalization and the addition of biocompatible coatings have been investigated, leading to a decrease in toxicity and environmental impact. Additionally, the ability to recycle these materials presents a considerable benefit. For example, magnetic iron oxide nanoparticles can be

efficiently retrieved from treated water through the application of external magnetic fields, allowing for their reuse across several cycles with negligible efficiency loss. Research indicates that doped metal oxides or composite structures enhance photocatalytic performance while also improving material stability, thereby supporting their reusability. Highlighting these features promotes a comprehensive understanding of the advantages and obstacles associated with the large-scale implementation of metal oxide nanostructures for water treatment.

## 6. Photocatalytic degradation of pesticides using metal oxide nanoparticles

The photocatalytic activity of metal oxide nanoparticles is attributed to their semiconducting properties, which enable efficient absorption of light and generation of electron-hole pairs. These properties are critical in driving the redox reactions required for environmental cleanup. These nano particles have an effective and selective photocatalytic activity due to their superconducting nature, which has been exploited in various



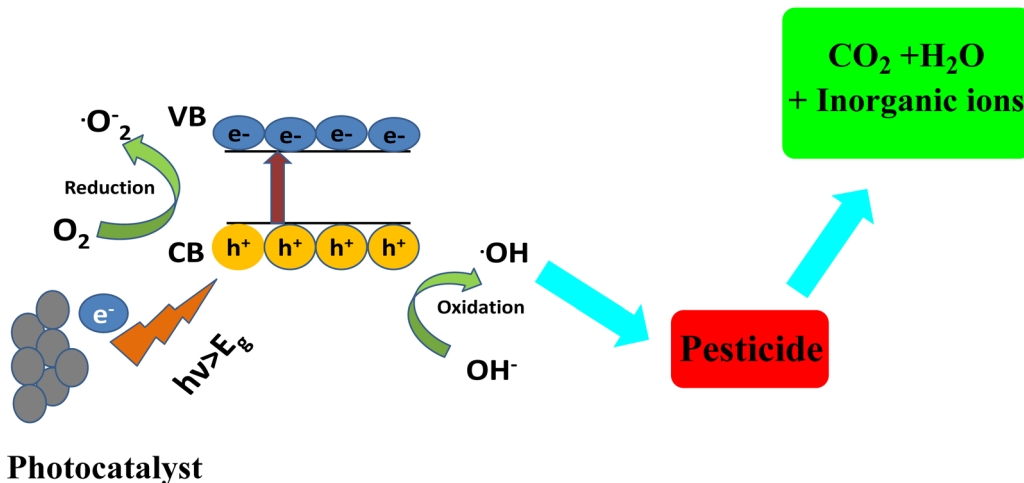


Fig. 3 Photocatalytic degradation of pesticides using photocatalysts.

research projects for pesticide sensing and remediation.<sup>56</sup> Metal oxide nano particles such as silica ( $\text{SiO}_2$ ), zinc oxide ( $\text{ZnO}$ ), titanium oxide ( $\text{TiO}_2$ ), and iron oxide ( $\text{Fe}_2\text{O}_3$  or  $\text{Fe}_3\text{O}_4$ ) have been utilized to detect, degrade, and remove pollutants from various sources.<sup>57,58</sup> The photocatalyst produces pairs of electrons and holes when it absorbs ultraviolet (UV) radiation from sunshine or artificially irradiated light sources (such as fluorescent lamps). When exposed to light radiation, the electron in the semiconductor catalyst's valence band becomes excited. This excited electron's extra energy aids in its transition to the catalyst's conduction band, where it leaves a positive hole behind. The result is the creation of the negative electron ( $e^-$ )

and positive hole ( $h^+$ ) pair. The term "photoexcitation" refers to this stage of the semiconductor catalyst. The "bandgap" energy is the difference in energy between the conduction band and the valence band. Fig. 3 illustrates the photocatalytic degradation of pesticides using the photo catalysts.

A recent analysis of the photocatalytic performance of metal oxide composites revealed that incorporating metals like silver and copper into structures such as  $\text{CuO}$  and  $\text{Fe}_2\text{O}_3$  extends the lifetime of electron-hole pairs.<sup>59,60</sup> This feature is crucial because it supports more efficient pesticide degradation under visible light exposure. The study showcased significant improvements in breaking down compounds like diazinon and

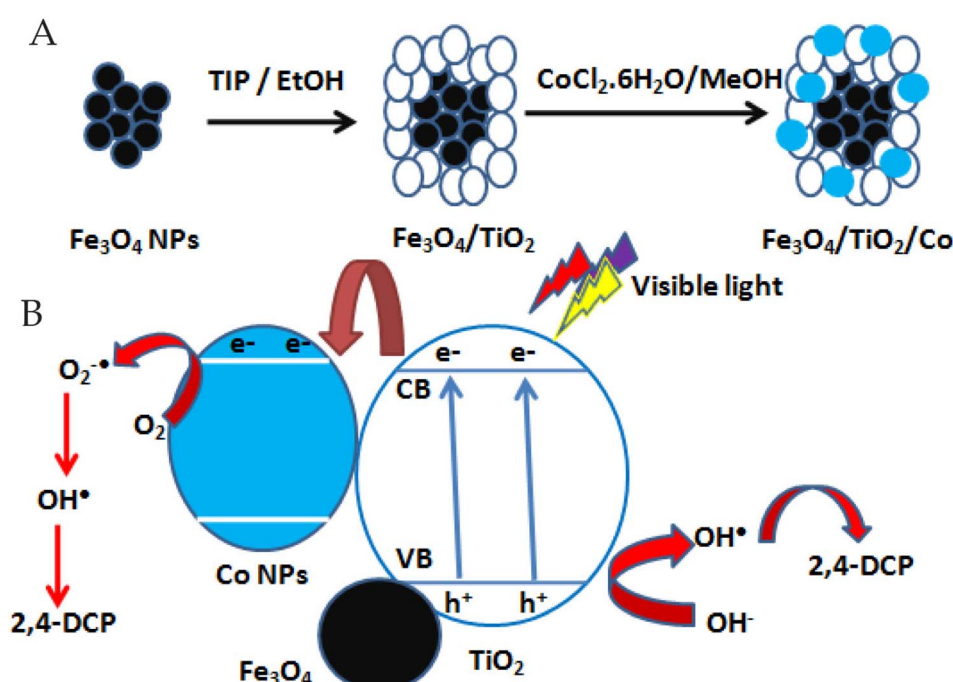


Fig. 4 2,4-Dichlorophenol degradation via photo-reactive  $\text{TiO}_2$  nanoparticles, (A) preparation of the photocatalyst; (B) the degradation pathway of 2,4-DCP.<sup>69</sup>

chlorpyrifos, underscoring how these structural modifications contribute to practical, sustainable solutions for environmental cleanup.<sup>61</sup>

### 6.1 Titanium oxide nanoparticles

$\text{TiO}_2$  has attracted the greatest attention from researchers because its unique characteristics, such as excellent photocatalytic activity across a wide range of pH and temperatures, cost-effectiveness, chemical stability, and non-toxicity.<sup>62</sup>  $\text{TiO}_2$  nanoparticles' high surface area for photocatalysis has allowed them to be used at the nanoscale to remediate a variety of pollutants from the environment.<sup>63</sup> With a bandgap of 3.2 eV,  $\text{TiO}_2$ 's photocatalytic activity is limited to the UV range.<sup>64</sup> On the other hand, dye sensitization and surface modification of  $\text{TiO}_2$  nanoparticles with other metal oxides, non-metals, or carbon-based compounds help to extend the photocatalytic activity of nanoparticles to the visible range.<sup>65</sup>  $\text{TiO}_2$  nanoparticles were used as a photocatalyst to degrade chlorpyrifos in water.<sup>66</sup> The photocatalyst was subjected to UV rays to produce pesticide degradation, and it was discovered that as the illumination period was increased, the photo-degradation efficiency rose.<sup>66</sup> To increase their photocatalytic activity against several pesticides,  $\text{TiO}_2$  nanoparticles have been treated with various metal ions. The fungicide carbendazim, for example, was destroyed by  $\text{TiO}_2$  nanoparticles doped with Fe and Si ions. The doping improved the photocatalytic activity of nanoparticles, resulting in a 98% breakdown of the fungicide in the presence of sunshine.<sup>67</sup> Also, during the advanced oxidation process (AOP), cobalt (Co)-doped  $\text{TiO}_2$  nanoparticles were used as a photocatalyst to decompose 2,4-dichlorophenol (DCP).<sup>68,69</sup> DCP was degraded by  $\text{TiO}_2$  nanoparticles in visible light because of the doping. They got 30.42% and 57.84% degradation of 2,4-DCP after 180 min irradiation in the presence of pure  $\text{TiO}_2$  and ternary nanocomposite containing 2.92 wt% cobalt ( $\text{Fe}_3\text{O}_4/\text{TiO}_2$  nanocomposite (2.92)), respectively. The higher photocatalytic performance of  $\text{Fe}_3\text{O}_4/\text{TiO}_2$

nanocomposite samples was attributed to the high specific surface areas and the enhancing visible light absorption by cobalt.<sup>69</sup> The pathway of 2,4-dichlorophenol degradation was illustrated in Fig. 4.

Recent studies have confirmed the enhanced photocatalytic properties of  $\text{TiO}_2$  doped with metals such as silver and iron, especially for degrading persistent organic pollutants like carbendazim,<sup>70</sup> tebuconazole (TEB) and 2,4-dichlorophenoxyacetic acid (2,4-D) pesticides.<sup>71</sup> Doping with silver, for example, has been shown to increase  $\text{TiO}_2$ 's reactivity under visible light, which reduces the energy needed for activation compared to pure  $\text{TiO}_2$ .<sup>71</sup> This is particularly significant because it allows for photocatalytic processes to occur under ambient light, making them more feasible for practical applications, including large-scale pollutant degradation.

Molecularly imprinted  $\text{TiO}_2$  photocatalysts were added so that the sol-gel method could be used to selectively remove certain pesticides from water.<sup>72</sup> Using  $\text{TiO}_2$  imprinted with the appropriate pesticide target, a notable improvement in photocatalytic performance was confirmed.<sup>73</sup> The comparison with the breakdown of pesticides that were not utilized as a template allowed for the verification of the photodegradation process's selectivity, as seen in Fig. 5.

It was looked into how adding foreign materials, like rare earth, transition, and noble metals, to  $\text{TiO}_2$  could increase the bathochromic shift, lower the band gap energy, and make photo-generated electron/hole pairs last longer.<sup>73</sup> Many surface parameters, including area, charge, and acidity, are altered by doping  $\text{TiO}_2$ , making the resulting material more photocatalytically active when exposed to visible light.<sup>73</sup> To make the rare earth lanthanide ions ( $\text{La}^{3+}$ ,  $\text{Nd}^{3+}$ ,  $\text{Sm}^{3+}$ ,  $\text{Eu}^{3+}$ ,  $\text{Gd}^{3+}$ , and  $\text{Yb}^{3+}$ )-doped  $\text{TiO}_2$  nanoparticles, the sol-gel method was used.<sup>74</sup> These were then tested as photocatalysts for dye remediation.<sup>75</sup> The shape, band gap, and particle size of  $\text{TiO}_2$  changed when lanthanides were added to it. This made the photocatalytic performance much better than pure  $\text{TiO}_2$ . The lowest bandgap,

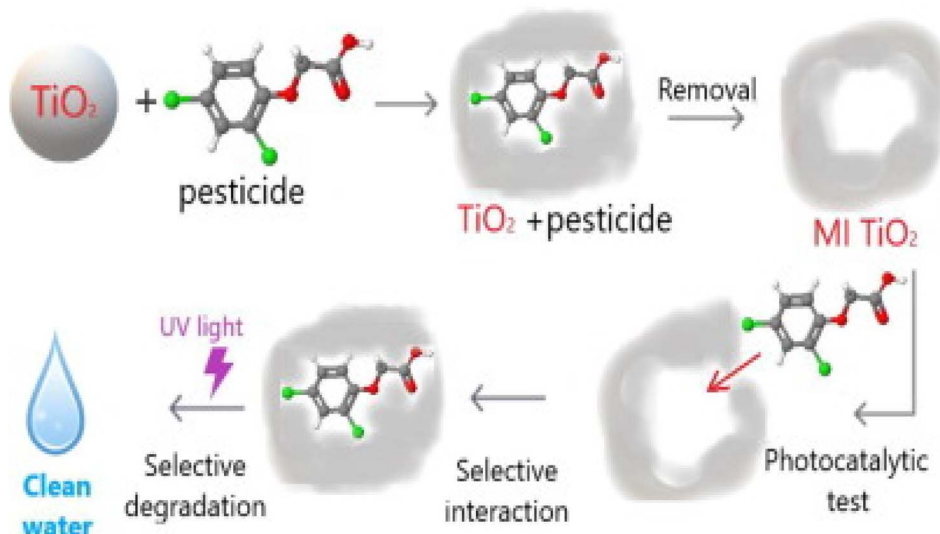


Fig. 5 Preferential removal of pesticides from water by molecular imprinting on  $\text{TiO}_2$  photocatalysts.<sup>73</sup>



Table 4  $\text{TiO}_2$  nanomaterials and their composites as photo-catalysts for pesticides degradation

Photo catalyst	Targeted pesticide	Light source	Reaction time	Degradation efficiency (%)	Ref.
$\text{TiO}_2/\text{Bi}_2\text{WO}_6$ nanostructured heterojunctions	4-Chlorophenol	Visible	7.5 h	90.5	77
$\text{TiO}_2/\text{Fe}_2\text{O}_3$ nanocomposite	Diazinon	Visible	45 min	95.1	78
$\text{Zn}^{2+}$ -doped $\text{TiO}_2$ nanoparticles	Malathion	UV	81 min	98	79
In and S co-doped $\text{TiO}_2@r\text{GO}$	Atrazine	Visible	20 min	99.5	80
SBA-15 loaded with 8–42% $\text{TiO}_2$	Dimethoate	Simulated solar	7 h	100	81

tiniest particle size with the greatest surface area, and pore volume of the lanthanides-doped  $\text{TiO}_2$  explained why the  $\text{Gd}^{3+}$  doping exhibited the highest photocatalytic performance.<sup>76</sup> The nanomaterials based on titanium dioxide and their composites for the photocatalytic destruction of some pesticides are compiled in Table 4.

## 6.2 Zinc oxide nanoparticles

Because of their distinctive size and high density at the surface's edge points,  $\text{ZnO}$  nanoparticles have unique chemical and physical properties.<sup>82</sup> These nanoparticles are also known to have high photocatalytic action, which is important for pollutant degradation. The band gap of zinc oxide is 3.25 eV, the same as that of  $\text{TiO}_2$  (3–3.25 eV).<sup>83</sup> It is often used in photocatalytic degradation processes to break down organic pollutants in wastewater. Photocatalytic process of zinc oxide and titanium dioxide are very similar. Because of this,  $\text{ZnO}$  nanoparticles have also been suggested as an alternative to titanium dioxide for cleaning water.  $\text{ZnO}$  performed better as a photocatalyst when compared to other semiconductors under investigation; this was due to  $\text{ZnO}$ 's ability to absorb a greater portion of the solar spectrum. It was also looked at how to employ  $\text{ZnO}$  nanoparticles' fluorescence emission properties for the photocatalytic destruction of various organic contaminants.<sup>84</sup> Because  $\text{ZnO}$ 's photocatalytic activity is extremely pH-sensitive and photo-corrosion is facilitated by strongly acidic conditions (pH

< 4), its potential is limited in lower pH media.<sup>85</sup> For the purpose of degrading the pesticide diazinon, the photocatalytic activity of nanocrystalline  $\text{ZnO}$  and commercially available  $\text{ZnO}$  was evaluated.<sup>86</sup> Nanocrystalline  $\text{ZnO}$  was found to have better photocatalytic activity than commercial  $\text{ZnO}$  because of two things: (a) its small crystalline size, which increased the active surface area of the photocatalytic reaction; and (b) the amount of dispersed  $\text{ZnO}$  particles per volume in the solution, which increased photon absorption for better performance.<sup>86</sup> Using natural sunlight to accelerate the photo-degradation of a variety of pesticides in the leaching water, the  $\text{ZnO}/\text{Na}_2\text{S}_2\text{O}_8$  nanocomposite was employed as an antioxidant and photosensitizer.<sup>87</sup> Adding  $\text{Na}_2\text{S}_2\text{O}_8$  to  $\text{ZnO}$  made it more effective at oxidation, which cut down on the time needed for photocatalytic pesticide breakdown.<sup>87</sup>

The  $\text{ZnO}-\text{SnO}_2$  nanorods are a potential material for water purification applications due to its great recyclability and facile remembrance of wasted photocatalysts.<sup>88</sup> Recent studies highlight the potential of  $\text{ZnO}$ -based photocatalysts for environmental cleanup, particularly when doped with transition metals or combined with nanocomposites.<sup>89</sup> For instance,  $\text{ZnO}$  doped with  $\text{Na}_2\text{S}_2\text{O}_8$  shows enhanced photocatalytic degradation of pesticides like diazinon, especially under natural sunlight in alkaline media, where its stability is higher.<sup>90</sup> In such conditions, the degradation rate can increase by up to 85%, demonstrating a significant improvement over pure  $\text{ZnO}$ . Similarly,

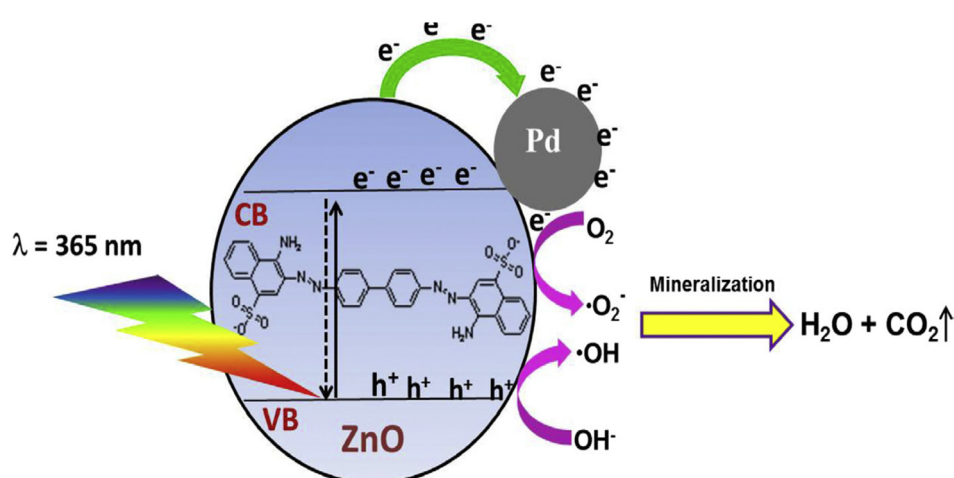


Fig. 6 Schematic diagram illustrating the plausible photocatalytic mechanism for degradation of Congo red dye using the Pd-doped  $\text{ZnO}$  photocatalyst.<sup>93</sup> Reprinted with permission from Copyright 2016 Elsevier.



Table 5 A summary of the ZnO and their composites that can break down pesticides through photocatalysis

Organic pollutant	ZnO-based nanomaterials	Light source	Degradation efficiency (%)	Ref.
Phenylhydrazine (PHZ)	ZnO supported onto clinoptilolite	UV-vis	69	95
2-Phenylphenol (OPP)	ZnO/TiO <sub>2</sub>	UV-vis	100	96
Diazinon	Nanocrystalline ZnO	UV-C	80	97
Azoxystrobin	ZnO/Na <sub>2</sub> S <sub>2</sub> O <sub>8</sub>	Sunlight	99	98
Hexaconazole			98	
Kresoxim-methyl			100	
Pirimicarb			95	
Propyzamide			97	
Pyrimethanil			96	

doping ZnO with manganese (Mn) improves photocatalytic efficiency by creating surface defects that promote electron–hole separation (ZnO's photocatalytic performance can be significantly improved by increasing its surface area, which reduces defects related to volume and enhances its ability to absorb more light. Studies have shown that doping ZnO with elements like manganese (Mn) or silver (Ag) can further enhance its photocatalytic activity by reducing electron–hole recombination.<sup>91,92</sup> This, in turn, increases the material's efficiency in degrading organic pollutants, making ZnO a more effective photocatalyst under visible light conditions), further boosting its ability to break down organic contaminants. This synergy between ZnO and its dopants or additives promises improved photocatalytic performance, making ZnO an effective solution for large-scale environmental remediation.<sup>86</sup>

Different methods were used to make the Pd-doped ZnO photocatalysts, and their ability to break down Congo red dye varied a lot. These methods included microwave irradiation, borohydride reduction, and photoreduction. Because of the higher doping and good dispersibility of Pd on ZnO, which improved the photodegradation efficiency of organic dye by reducing the recombination of photogenerated electron–hole pairs, the Pd-doped ZnO photocatalyst prepared by the borohydride reduction method exhibited superior photocatalytic activity (Fig. 6).<sup>93</sup> Er-doped ZnO nanoparticles with varying Er concentrations increased photocatalytic activity when exposed to visible light. Adding different amounts of Er to ZnO nanoparticles changed their structure, morphology, band gap, half-life of the photogenerated electron–hole pair, and their ability to absorb visible light. This doped ZnO was used to degrade Red-31 dye.<sup>94</sup> A summary of the ZnO and their composites that can break down pesticides through photocatalysis is shown in Table 5.

### 6.3 Iron oxide nanoparticles

The n-type semiconductor iron oxide is widely accessible and could break down organic contaminants through photocatalysis.<sup>99</sup> Moreover, the inherent magnetic effect facilitates the material's easy recovery from the aqueous medium, making it a viable photocatalytic material.<sup>99</sup> Fe<sub>2</sub>O<sub>3</sub> semiconductors were found to be activated by visible light because of their low band gap energy (2.2 eV).<sup>100</sup> Recent work has shown that gold-doped iron oxide (Fe<sub>2</sub>O<sub>3</sub>) nanoparticles enhance photocatalytic

efficiency for degrading organic dyes. For example, in the degradation of Disperse Blue 79, photocatalytic efficiency improved by 35% when Fe<sub>2</sub>O<sub>3</sub> was doped with 1% gold.<sup>101</sup> However, challenges remain, such as the rapid recombination of electron–hole pairs and the need for longer reaction times. These limitations must be addressed to optimize large-scale applications in wastewater treatment and pollutant degradation.

The degrading properties of Fe<sup>3+</sup> oxides under photocatalysis, including  $\alpha$ -Fe<sub>2</sub>O<sub>3</sub>,  $\gamma$ -Fe<sub>2</sub>O<sub>3</sub>,  $\alpha$ -FeOOH,  $\beta$ -FeOOH, and  $\gamma$ -FeOOH, were examined with the purpose of destroying harmful organic pollutants within the visible spectrum of the sun.<sup>102</sup> Low-band-gap iron oxide nanoparticles can be applied to photocatalytic reactions that occur within the visible portion of the solar spectrum.<sup>103</sup> The quick recombination of the photo-generated electron–hole pair, however, poses a significant obstacle to their viability in photocatalytic uses (Fig. 7).<sup>104</sup>

The recombination events of charge carriers are tuned, and the photocatalytic activity is enhanced through the doping of iron oxide nanostructures with varying metals or metal oxides and the construction of iron oxide-based nanocomposites. When exposed to sunlight, Au-Fe<sub>2</sub>O<sub>3</sub> aerogels with different amounts of Au were tested as photocatalysts for breaking down the dye Disperse Blue 79. The metallic gold made Fe<sub>2</sub>O<sub>3</sub> more photocatalytic by allowing more photogenerated electrons to build up and delaying the recombination process. So, oxidative species backed by photogenerated charge carriers attacked the azo dye molecules that had stuck to the surface.<sup>105</sup> Iron oxide-based photocatalysts are promising options for the removal of organic pollutants from wastewater due to their high recycling value, inexpensive cost, and practicality. Controlling the size, shape, and surface properties of iron oxide NPs, which play a key role in the detection and destruction of a variety of agro-chemicals, can improve the efficacy and specificity of pesticide remediation operations.

### 6.4 Silica nanoparticles

Silica-based materials have received considerable interest in pesticide degradation owing to their elevated surface area, adjustable porosity, and chemical stability.<sup>106</sup> These characteristics render silica a superior support material for catalytic and photocatalytic applications. Using advanced oxidation processes, different active species, such as titanium dioxide or



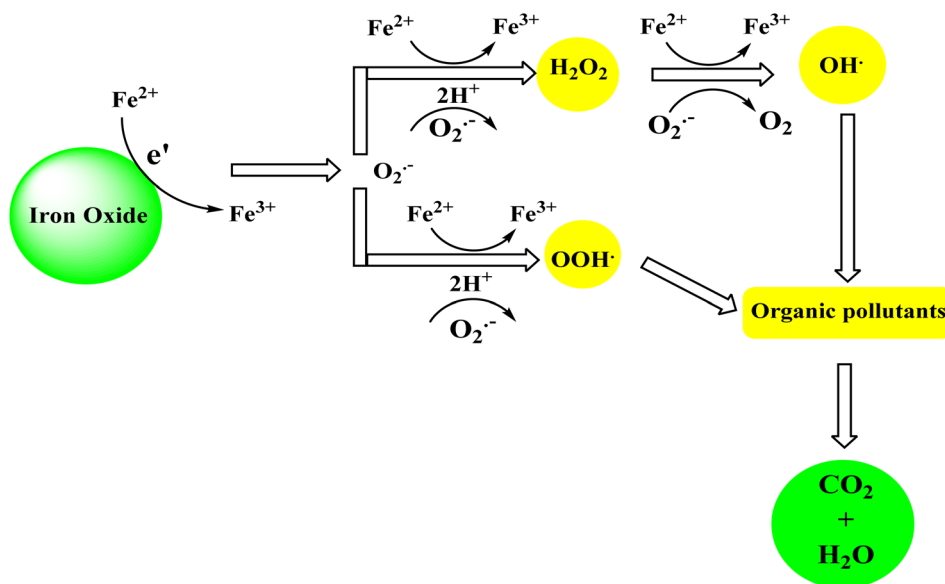


Fig. 7 Photo-degradation pathways for organic pollutants using iron oxide.

transition metal oxides, can be added to silica to make pesticides break down more quickly. Additionally, the biocompatibility and environmental safety of silica make it a favorable choice for sustainable applications. Nonetheless, the application of silica in pesticide degradation presents certain limitations.<sup>107</sup> The synthesis of functionalized silica materials is complex and costly, which may restrict large-scale applications. Silica by itself usually doesn't have much catalytic activity, so it needs to be changed with active agents. If this isn't done properly, it can cause problems for the environment. The regeneration and reuse of silica-based catalysts present challenges, as fouling or activity loss over multiple cycles may diminish their economic viability. Ongoing advancements in material science are enhancing silica's effectiveness in pesticide degradation, despite existing limitations. The integration of nano-engineered features has demonstrated potential in addressing several of these challenges.<sup>108</sup> Recent research highlights the significant role of silica nanoparticles ( $\text{SiO}_2$  NPs) in environmental remediation, particularly in the extraction and degradation of pesticides.<sup>109</sup> The unique properties of  $\text{SiO}_2$  NPs, such as their high surface area and tunable porosity (microporous, mesoporous, or hollow), make them ideal candidates for sorbent materials in solid-phase extraction (SPE) techniques. For instance,  $\text{SiO}_2$  NPs functionalized with *N*-methylimidazole have demonstrated a remarkable ability to adsorb polar pesticides such as sulfonylurea from aqueous samples, with extraction efficiencies reaching up to 85%.<sup>110</sup> Similarly, when co-functionalized with polar cyanopropyl-triethoxysilane (CNPrTEOS) and non-polar methyltrimethoxysilane (MTMOS),  $\text{SiO}_2$  NPs have been successfully used to extract a variety of organophosphate pesticides, including diazinon, methidathion, and chlorpyrifos, from water samples, achieving extraction efficiencies exceeding 90%.<sup>111</sup> These pesticides were then quantified using high-performance liquid chromatography (HPLC) and gas chromatography-mass

spectrometry (GC-MS) for precise analysis. Furthermore, silica molecular imprinted polymers (MIPs) made from  $\text{SiO}_2$  NPs have been shown to enhance pesticide extraction, as demonstrated by significant increases in fluorescence or chemiluminescence intensity in response to pesticide concentrations.<sup>112,113</sup>

## 6.5 Cerium oxide

The potential uses of cerium dioxide (ceria) include fuel cell reformer, hydrocarbon fuel oxidation, and photocatalytic degradation of organic pollutants due to its non-toxicity, high thermal stability, specific chemical reactivity, and rigidity.<sup>114,115</sup> In addition to its exceptional catalytic capabilities, the ceria displays a broad band gap of 3.1 eV.<sup>116</sup> Several organophosphate pesticides have been photodegraded using it.<sup>117,118</sup> The temperature at which ceria is calcined has a significant impact on its photocatalytic capability. Organophosphate pesticides effectively adsorb on the surface of ceria by electrostatic contact with the hydroxyl functions of ceria nanoparticles because of their positive charge on phosphorus. The ceria nanoparticles calcined at a lower temperature effectively adsorb organophosphate insecticides, which photo-catalyzed to break them down.<sup>119</sup> It was shown that  $\text{CeO}_2-\text{Fe}_2\text{O}_3$  composites were magnetically separable and could break down organophosphate insecticides quickly.<sup>120</sup> The  $\text{CeO}_2-\text{Fe}_2\text{O}_3$  composite that was calcined at a temperature of 300–400 °C demonstrated the maximum degrading efficiency and kept its good magnetic characteristics, enabling simple separation. The  $\text{CeO}_2-\text{Fe}_2\text{O}_3$  site was calcined at a temperature greater than 500 °C, which greatly reduced its surface area, active surface sites, and pore volume while concurrently increasing its crystallinity. At high calcination temperatures, these modifications decreased the photocatalytic activity of the  $\text{CeO}_2-\text{Fe}_2\text{O}_3$  composite. When compared to commercially available  $\text{CeO}_2$  nanoparticles, one-dimensional  $\text{CeO}_2$  nanotubes ( $\text{CeO}_2$ -NT) with a hollow interior

demonstrated improved photocatalytic degradation of phenols.<sup>121</sup> Researchers found that the  $\text{CeO}_2$  nanotubes' higher photocatalytic activity compared to the nanoparticles was since the photocatalytic behavior of ceria changes depending on its shape. It was shown that the  $\text{CuO}-\text{CeO}_2$  catalyst could degrade methyl orange dye more effectively in the microwave, both with and without  $\text{H}_2\text{O}_2$ .<sup>122</sup> The process of organic pollutants photo-degradation is accelerated by the hydroxyl radicals generated by  $\text{H}_2\text{O}_2$ . Rhodamine B dye was degraded by  $\text{CeO}_2-\text{Y}_2\text{O}_3$  binary metal oxide nanostructures with a changeable molar ratio under UV-visible light, and the degradation efficiency was 98%.<sup>123</sup> The photocatalytic degradation of the  $\text{CeO}_2-\text{Y}_2\text{O}_3$  nanocomposites was much better than that of the  $\text{CeO}_2$  and  $\text{Y}_2\text{O}_3$  components alone. Increased oxygen vacancies and a large active surface area were credited with the improved photocatalytic activity. The higher pH and  $\text{H}_2\text{O}_2$  speeds up the photo-degradation reactions by removing electrons from the conduction band and making more hydroxyl radicals.<sup>123</sup>

## 6.6 Copper oxides

With band gap energy of about 1.4 eV, copper oxides are cheap, widely accessible and environmentally benign p-type semiconductor materials.<sup>124</sup>  $\text{CuO}$ 's tiny band gap makes it possible to absorb visible light, which is necessary for photocatalytic activation. There are two main types of copper oxide:  $\text{CuO}$  and

$\text{Cu}_2\text{O}$ .  $\text{CuO}$  has been discovered to have better photocatalytic activity than  $\text{Cu}_2\text{O}$ . The narrow bandgap energy, which promotes recombination of these pairs, hinders the photo-generated electron–hole pairs' potential for photocatalytic applications. Copper oxide nanoparticles have recently been functionalized or doped with different metal oxides (like  $\text{TiO}_2$ ,  $\text{ZnO}$ ,  $\text{SiO}_2$ , *etc.*),  $\text{MoS}_2$ , ionic liquids, reduced graphene oxide, and other things to make them better photocatalytic.<sup>125</sup> These modifications have changed the electronic structure, light absorption characteristics, and charge transport characteristics.<sup>126</sup>

The hierarchical 3D metal oxide– $\text{CuO}$  nanostructures containing  $\text{ZnO}$  and  $\text{Fe}_3\text{O}_4$  improved the photocatalytic properties for the breakdown of Congo red dye under solar light.<sup>127</sup> This might be because the n-type ( $\text{ZnO}/\text{Fe}_3\text{O}_4$ ) and p-type ( $\text{CuO}$ ) semiconductors have better charge separation at the p–n junction, which is where the two types of semiconductors meet (Fig. 8).<sup>127</sup> The band gap of pure  $\text{CuO}$  nanowires was changed by making hetero-architectural composites of  $\text{Fe}_3\text{O}_4-\text{CuO}$  (1.7 eV) and  $\text{ZnO}-\text{CuO}$  (1.5 eV), which have lower band gap energies than pure  $\text{Fe}_3\text{O}_4$  (2.19 eV) and  $\text{ZnO}$  (3.34 eV), respectively.<sup>128</sup>

Doping  $\text{ZnO}$  with  $\text{CuO}$  leads to stoichiometric deficiencies and structural flaws in the nanomaterial. These flaws change the band gap energy and make the  $\text{CuO}-\text{ZnO}$  nanocomposite more photocatalytic. Additionally, the presence of exogenous electron acceptors—specifically,  $\text{H}_2\text{O}_2$ , peroxomonosulfate, and

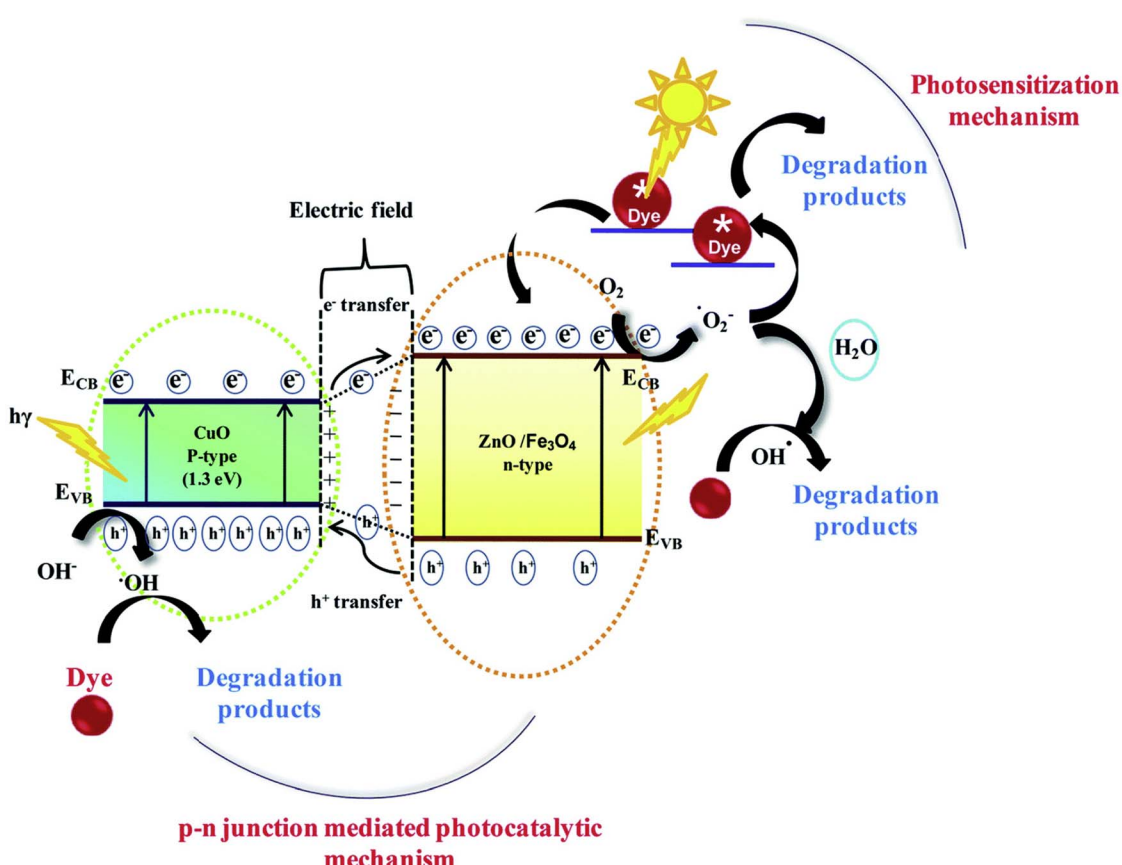


Fig. 8 Photocatalytic degradation pathway under the solar light irradiation using the p–n heterojunctions ( $\text{ZnO}-\text{CuO}$  or  $\text{Fe}_3\text{O}_4-\text{CuO}$ ).<sup>127</sup> Copyright 2016 Elsevier.



peroxodisulfate—improved the photocatalytic degradation of textile dyes.<sup>129</sup> When exposed to visible light, the p-n junction-type semiconductor CuO-TiO<sub>2</sub> displayed good photocatalytic activity and broke down the azo dyes on the CuO-TiO<sub>2</sub>-zeolite. Under visible light, CuOTiO<sub>2</sub>-zeolite breaks down 90% of the methylene blue dye in 60 minutes, while zeolite, TiO<sub>2</sub>-zeolite, and CuO-zeolite could remove 79.1%, 84.1%, and 85.2% of the dye, respectively, under the same circumstances. The photocatalytic activity under visible light exposure was boosted by bandgap engineering, active surface area-driven suppression of charge carrier recombination, and improved interfacial charge transfer.

### 6.7 Other metal oxides

Different metal oxides and their composites have also been able to photocatalytically degrade a variety of organic contaminants. The large band gap (3.6 eV) of the n-type semiconductor SnO<sub>2</sub> favors many photocatalytic processes.<sup>130</sup> Functionalizing SnO<sub>2</sub> with MgO prevented the recombination of photogenerated electrons and holes, enhancing the SnO<sub>2</sub>-MgO nanocomposite's photocatalytic abilities. SnO<sub>2</sub>-MgO nanocomposites have demonstrated the ability to photocatalytically degrade textile colorant compounds.<sup>131</sup>

It was shown that the hetero-structure of Fe<sub>2</sub>O<sub>3</sub>-WO<sub>3</sub>, WO<sub>3</sub>-TiO<sub>2</sub>, and MoO<sub>3</sub>-TiO<sub>2</sub> nanocomposites significantly improved the photocatalytic degradation.<sup>132,133</sup> The photocatalytic properties were improved by the n<sup>+</sup>-n heterojunction of the rhombohedral  $\alpha$ -Fe<sub>2</sub>O<sub>3</sub> nanoparticles that were spread out evenly on the surface of the monoclinic WO<sub>3</sub> structures. The potential energy difference between Fe<sub>2</sub>O<sub>3</sub> and WO<sub>3</sub> facilitates the separation of photogenerated charge carriers, which in turn enhances the photocatalytic destruction of organic contaminants (Fig. 9).<sup>132</sup> The p-n heterojunction structure of the Co<sub>3</sub>O<sub>4</sub>/BiVO<sub>4</sub> combination made it last a long time and destroy organic pollutants effectively through photocatalysis.<sup>134</sup> A decrease in the recombination rate of photogenerated charge carriers,

according to photoluminescence research,<sup>134</sup> is what led to the increased photocatalytic activity.

Bi<sub>2</sub>O<sub>3</sub> is a non-toxic p-type semiconductor with a band gap of 2.8 eV and a greater valence hole oxidation power.<sup>135</sup> It has gotten more attention because it breaks down different dyes. The pharmaceutical component acetaminophen (APAP) has been photodegraded using highly crystalline monodisperse  $\beta$ -Bi<sub>2</sub>O<sub>3</sub> nanospheres.<sup>136</sup> A direct-hole oxidation method was suggested to break down APAP. The oxidation process produced comparatively fewer intermediates, which were linked to the high oxidation power of  $\beta$ -Bi<sub>2</sub>O<sub>3</sub> nanospheres that had high mineralization efficiency. However, because of the quick recombination of electron-hole pairs produced by visible light, pure Bi<sub>2</sub>O<sub>3</sub> exhibits limited photocatalytic efficiency. Adding transition metals or their oxides to Bi<sub>2</sub>O<sub>3</sub> made it much better at breaking down organic pollutants through photocatalysis.<sup>136</sup> Matsumura *et al.* studied 2% Ce- and 1.5% Nd-doped Bi<sub>2</sub>O<sub>3</sub> nanorods to see how they would break down organic dyes like Acid Yellow 29, Coomassie Brilliant Blue G250, and Acid Green 25.<sup>137</sup> They made it clear that the dopants can easily grab the photogenerated electrons from Bi<sub>2</sub>O<sub>3</sub>'s conduction band. This slows down the recombination process and increases the photocatalytic activity of the nanomaterials.

## 7. Pesticides adsorption using metal oxide nanoparticles

Adsorption is the physicochemical surface interaction between the adsorbate and the adsorbent.<sup>138</sup> Temperature, adsorbent-adsorbate interaction forces, medium pH, the presence of foreign components, concentration, and other parameters all affect the adsorption process.<sup>139</sup> Adsorbents should have a large surface area, adequate textural and surface characteristics, and sufficient mechanical stability to remove pesticides from wastewater quickly and efficiently.<sup>140</sup> Organic contaminants in wastewater act as adsorbates, slowly absorbing on adsorbent surfaces until an equilibrium between adsorbent and adsorbate is achieved.<sup>141</sup> Adsorption isotherms of many forms have been created to better understand the adsorption mechanism. Adsorption can be classified as chemisorption or physisorption depending on how they interact with the adsorbates.<sup>141</sup>

In physisorption, a physical interaction through which adsorbable molecule (the adsorptive) is adsorbed onto (surface physisorption) or into (intercalation) the metal oxide and their composites (adsorbent), through van der Waals forces, hydrogen bonding, or dipole-dipole attraction.<sup>141</sup> It falls into three general categories. The most well-known is pure physical adsorption, which is represented as full adsorbate recovery either with an increase in temperature or a drop in the concentration of the surrounding medium. It is a low-temperature phenomenon since the interaction forces get less as the temperature rises.<sup>142</sup> The second category, active adsorption, is characterized by complex formation leading to a partial recovery of the adsorbate. It is a high-temperature process that breaks down complexes above a particular temperature, after which they reach equilibrium.<sup>143</sup> The third

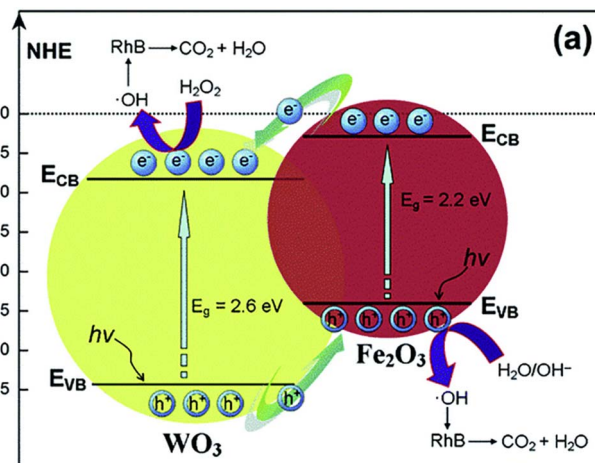


Fig. 9 Mechanism pathway of light-induced charge separation in the Fe<sub>2</sub>O<sub>3</sub>-WO<sub>3</sub> nanocomposite and photo-degradation of Rhodamine B.<sup>132</sup> Copyright 2014 Royal Society of Chemistry.



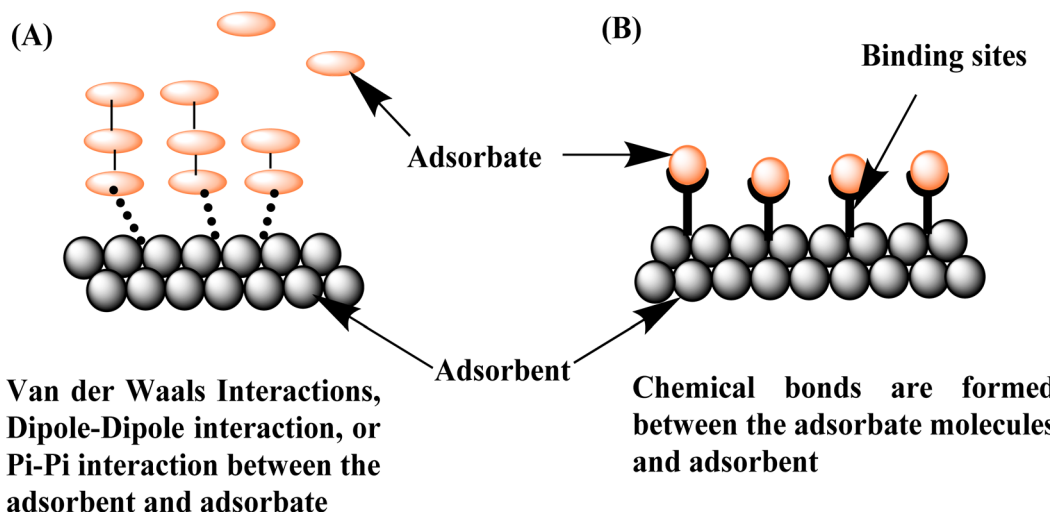


Fig. 10 The adsorption process in: (A) multiple layers (physisorption); and (B) single (chemisorption).

Table 6 Iron oxide-based nanomaterials and their composites as adsorbents for the removal of some pesticides

Adsorbent	Structure	Pesticide	Adsorption removal (%)	Ref.
Fe <sub>3</sub> O <sub>4</sub> @nSiO <sub>2</sub> @mSiO <sub>2</sub>	Core-shell microspheres	DDT	97%	159
MWCNTs/iron oxide/β-CD	Magnetic microspheres	<i>p</i> -Nitrophenol	69.6%	160
Mg/Al double layered hydroxide	Nanocrystalline particles	Humic acid	98.8	161
		Fulvic acid	97.6	

category is solution, in which the adsorbate is lost through diffusion and is not recovered in the adsorbent core. Chemisorption, in contrast to physisorption, is an adsorption process in which a modifying molecule (the adsorptive) and a surface (the adsorbent) make a chemical connection.<sup>144</sup> Chemisorption occurs either by radical processes or by ionic phenomena.<sup>145</sup> For further explanation, adsorption details are explained in Fig. 10 in both single and multiple-layer models.

The combination of various materials with diameters in the nanoscale range is called a nanocomposite. Combining the qualities of various materials to create a unique nanomaterial with enhanced and better chemical and physical capabilities is the goal of creating nanocomposites. The characteristics of the raw materials and the nanocomposites are very different. In comparison to conventional composite materials, nanocomposites have a huge surface area and a great surface-to-volume ratio.<sup>146</sup> In the realm of environmental studies, these composite materials have garnered interest, particularly for the removal of pesticides from various samples.<sup>147</sup> The main cause of this is the variety and special qualities that the nanomaterials provide, helping with the pesticide removal process. A nanotube is a long, hollow, tubular nanomaterial with a diameter that typically ranges in nanometers and a length that can vary from nm to mm. Because of their high aspect ratio and huge surface area, nanotubes can be used as effective adsorbents for a variety of chemicals. For a variety of uses, different materials, including enzymes, medications, hormones, and nucleic acids, have been entrapped in the lumen of these nanotubes and

bonded to their surface. Because of their special qualities and vast surface area, carbon nanotubes (CNTs) and halloysite nanotubes (HNTs) have garnered a lot of interest in the field of environmental remediation.

## 7.1 Iron oxides

Among the elements that are most prevalent in the crust of the earth is iron. It has a wide range of oxidation states and is quite reactive. The oxidation state and chemical composition of iron determine the crystalline and structural characteristics of iron oxide nanoparticles. The major oxide forms of iron are magnetite ( $Fe_3O_4$ ), maghemite ( $\gamma-Fe_2O_3$ ), and hematite ( $\alpha-Fe_2O_3$ ).<sup>148</sup> The commonly utilized iron oxide nanoparticles, magnetite, include two separate forms of iron in distinct oxidation states:  $Fe^{2+}$  and  $Fe^{3+}$ . Iron oxide particles' nano-dimension offers super-paramagnetism and a high surface-area-to-volume ratio. Iron oxide nanoparticles have gotten a lot of attention for a wide range of uses because they are easy to make and change the surface of, they are easy to find, they have unique properties at the nanoscale level, they can separate magnetically, and they are not toxic.<sup>149</sup> For the adsorption of organic contaminants, iron oxide nanoparticles in their pure, doped, and composite forms have been widely employed.<sup>150</sup> After organic pollutants were adsorbed, separating the spent adsorbent from the wastewater has proven to be a significant challenge that calls for energy-intensive procedures like centrifugation. Even so, spent iron oxide-based adsorbents (after removing organic contaminants) are easily separated





Table 7 Titanium dioxide and their composites as adsorbents for the removal of pesticides from the wastewater

Adsorbent	Structure	Pesticides	Adsorbent amount	Contact time	Adsorption removal (%)	Ref
Nano-PP/TiO <sub>2</sub>	Nano-polypropylene–titanium dioxide	Malathion	0.5 g L <sup>-1</sup>	52 min	96	166
Cellulose/PAN/TiO <sub>2</sub>	Cellulose/polyaniline/TiO <sub>2</sub> photocomposites	Acetamiprid	—	—	99	167
Nano-PP/TiO <sub>2</sub>	Nano-polypropylene–titanium dioxide	Organophosphorous	2.25 g L <sup>-1</sup>	32.2 min	69.3	168
Fe <sub>3</sub> O <sub>4</sub> @SiO <sub>2</sub> @MOF/TiO <sub>2</sub> nanocomposite	Magnetic metal–organic framework–titanium dioxide nanocomposite	Fungicides (triadimenol, hexaconazole, diniconazole, myclobutanil, and tebuconazole)	—	—	93–95	169

when there is an outside magnetic field.<sup>151</sup> Iron oxide nanoparticles and their composites are therefore becoming more and more popular for use in wastewater treatment applications.<sup>151</sup>

Iron oxide (magnetite) nanoparticles were used to effectively remove chlorinated pesticides such as dieldrin, 2,4-dichlorophenoxyacetic acid (2,4-D), 2,4,5-trichlorophenoxyacetic acid (2,4,5-T), lindane (1,2,3,4,5,6-hexachlorocyclohexane), and hexachlorocyclohexane ( $\alpha$ -HCH and  $\gamma$ -HCH) from the polluted water.<sup>152,153</sup> Their chemical structure determines how they adsorb on the iron oxide nanoparticles. Adding surfactants or surface-acting agents to the surface of iron oxide nanoparticles can make them better at absorbing things and being selective.<sup>154</sup> Much work has recently been done on the surface functionalization of iron oxide nanoparticles using a variety of organic species and functionalities, including polyacrylic acid, glutamic acid, organosilane, and so forth. An easy-to-use and practical method for separating used adsorbents must be combined with adsorption properties. The magnetic core of Fe<sub>3</sub>O<sub>4</sub>, the layer of nonporous silica (nSiO<sub>2</sub>), and the layer of mesoporous silica (mSiO<sub>2</sub>) on the outside of the magnetic mesoporous Fe<sub>3</sub>O<sub>4</sub>@nSiO<sub>2</sub>@mSiO<sub>2</sub> nanoparticles showed a high rate of adsorption and the ability to remove the pesticide DDT.<sup>155</sup>

The immobilized Fe<sub>2</sub>O<sub>3</sub> NPs considerably improved palygorskite's ability to retain phenarimol. According to Ouali *et al.*,<sup>156</sup> the material's adsorption capacity demonstrated stability over a two-week period, suggesting a wider application of this material for the long-term elimination of fenarimol. Using a similar strategy, iron oxide nanoparticles (NPs) trapped in mesoporous silica have been used to extract glyphosate from water. Immobilization significantly increased the magnetic adsorbent's surface area and porosity.<sup>157</sup> Fan *et al.*, used Fe<sub>3</sub>O<sub>4</sub> nanoparticles and a simple, quick, and sensitive liquid–liquid extraction method to get rid of pyrethroid pesticides from tap, pond, river, and lake water, among others. Four types of pyrethroids were eliminated from water samples.<sup>158</sup>

In conclusion, changing the NPs' size, shape, and surface properties—which are important for finding and getting rid of different agrochemicals—can make these methods that use iron oxide NPs for pesticide cleanup more effective and selective. Because of how they are made, iron oxide nanoparticle surface modifications and mixing them with other nanomaterials will speed up the breakdown and removal of pesticides. Table 6 summarizes the performance of iron oxide-based nanomaterials and their composites as adsorbents for the removal of some pesticides.

## 7.2 Titanium oxide

Due to its favorable zero point charge (pH<sub>pzc</sub> = 6–6.8), controlled structural and textural features, high surface reactivity, easy synthesis, and abundant availability of precursors, titanium dioxide (titania) nanomaterials have been investigated as an adsorbent.<sup>152</sup> Additionally, titanium functions as a photocatalytic substance to convert dangerous chemical molecules into harmless ones.<sup>162</sup> One of the most important conditions for

Table 8 Zinc oxide and their composites as adsorbents for the removal of pesticides from the wastewater

Adsorbent	Structure	Pesticide	Adsorption removal (%)	Ref.
CPZiONp-composite	Cucumber peels-zinc oxide nanoparticles composite	Metribuzin	66	172
CS-ZnONPs	Chitosan-zinc oxide nanoparticles	Permethrin	99	173
ZnO-Np	Zinc oxide nanoparticles	Simazine	72	174
ZnO-AC	ZnONP-doped activated carbon	Glyphosate	98	175

Table 9 Silicon dioxide and its composites as adsorbents for the removal of pesticides from the wastewater

Adsorbent	Structure	Pesticide	Adsorption removal (%)	Ref.
SiO <sub>2</sub>	Silica nanoparticles	Azoxystrobin	95.21	181
SiO <sub>2</sub>	Silica nanoparticles	Cypermethrin	88	182
Ni@SiO <sub>2</sub> -G	Nickel@silica-graphene nanocomposites	Organothiophosphate	99	183
PAni:PPy@SiO <sub>2</sub>	Polyaniline and polypyrrole with silicon dioxide	2,4-Dichlorophenol	97	184

the photodegradation of organic contaminants is their adsorption on the titania surface. The adsorption of organic pollutants facilitates the interface between the pesticide molecules and surface-active species, or photo-excited holes, and this starts the photo-oxidation events.<sup>163</sup> As a result, the adsorption effectiveness of the titania nanostructure controls the photo-degradation of organic contaminants. Titania's surface properties are influenced by the size, shape, crystallinity, and phase composition of the particles, which in turn affect the adsorption and photocatalytic destruction of organic contaminants. After being manufactured using a hydrothermal technique, the hierarchical nanostructured TiO<sub>2</sub>, or TiO<sub>2</sub> 1D nanorods, TiO<sub>2</sub> 3D0D microspheres, and TiO<sub>2</sub> 3D1D microspheres, showed morphological feature-dependent photocatalytic degradation of phenol. Compared to the 1D nanostructured equivalent, the organic pollutants degraded more quickly and efficiently in the hierarchical 3D nanostructured TiO<sub>2</sub> due to its larger degree of surface-active sites and desirable band gap energy.<sup>164</sup>

Six organochlorine pesticides were micro-extracted using mesoporous TiO<sub>2</sub> NPs.<sup>165</sup> These are hexachlorobenzene (HCB), *trans*-chlordane, *cis*-chlordane, *o,p*-DDT, *p,p*-DDT, and mirex. To remove the pesticides, solid-phase micro-extraction fiber was created using the NPs. Additionally, the produced fiber was utilized to find these chemicals in samples of lake and rainwater.<sup>156</sup> This enhanced adsorption is due to surface charge interactions and hydrogen bonding between the titanol groups of the aerogel and molecules' aromatic rings, nitrogen, and oxygen groups. The ability of the titania aerogel to regenerate adsorption sites at higher pH levels indicates its promise as a durable and efficient adsorbent for environmental cleanup.<sup>152</sup> Table 7 shows TiO<sub>2</sub> and their composites as adsorbents for the removal of pesticides from the wastewater.

### 7.3 Zinc oxides

ZnO NPs have distinct chemical and physical characteristics because of their high density at the surface's edge points and

size. Additionally, these NPs have demonstrated strong photocatalytic activity, which is crucial for the breakdown of contaminants. Zinc oxide nanoparticles' surface functionalization improves both their catalytic and sensing capabilities. In a reported research study, it reveals that the adsorption capacity depends not only on the textural features of the material but also on the functionalization of the nanoparticles. It was found that 1-butyl-3-methylimidazolium tetrafluoroborate (BMTF-IL) functionalized zinc oxide nanoparticles show maximum adsorption capacity (148.3 mg g<sup>-1</sup>) towards naphthalene removal as compared with CTAB functionalized (89.96 mg g<sup>-1</sup>) and bare ZnO (66.80 mg g<sup>-1</sup>) nanoparticles.<sup>170</sup>

Using ZnO NPs, permethrin—a neurotoxic insecticide that is frequently used in agriculture—was eliminated from the water sample. To create beads for the effective removal of the pesticide, NPs and chitosan were mixed. At room temperature and neutral pH, the pesticide's maximum removal efficacy (99%) was achieved using 0.5 g of beads. After three cycles, the beads showed themselves to be a promising material for treating water, with a 56% regeneration effectiveness.<sup>171</sup> Table 8 shows ZnO and their composites as adsorbents for the removal of pesticides from the wastewater.

### 7.4 Silicon dioxide

The spherical, porous particles known as silica nanoparticles (SiO<sub>2</sub> NPs) can be produced chemically or biologically.<sup>176</sup> Depending on the manufacturing conditions, the particles' porosity can be hollow, mesoporous, or microporous.<sup>177</sup> These particles can conjugate with a variety of chemical and biological substances by undergoing physical and chemical modification. Several environmental contaminants have been remedied using these NPs.<sup>178</sup> They have been applied to various pesticide detection, degradation, and extraction processes.

Pesticides have been extracted from a wide range of materials using solid-phase extraction (SPE). Owing to their substantial surface area, SiO<sub>2</sub> NPs are typically employed in the



Table 10 Silicon dioxide and its composites as adsorbents for the removal of pesticides from the wastewater

Adsorbent	Structure	Pesticide	Adsorption removal (%)	Ref.
MgO NPs	Magnesium oxide nanoparticles	Thiamethoxam	60.13	188
		Chlorpyriphos	80.53	
		Fenpropathrin	92.49	
MTBC	Triadimefon & dinotefuran	Triadimefon	86.42	189
		Dinotefuran	87.86	
MgO/Fe <sub>3</sub> O <sub>4</sub> -synthesized porous carbons	MgO/Fe <sub>3</sub> O <sub>4</sub> modified coconut shell biochar	Atrazine	90.24	190
MgFe <sub>2</sub> O <sub>4</sub>	Mesoporous magnesium ferrite	Chlorpyrifos	91	191

production of sorbents for use in SPE techniques. These NPs' effectiveness and pesticide selectivity are increased when their surfaces are modified. SiO<sub>2</sub> NPs were used to extract sulfonylurea from water samples after they were functionalized with *N*-methylimidazole. Functionalization improved the polar pesticide's ability to bind to NP surfaces.<sup>179</sup> SiO<sub>2</sub> nanoparticles have also been used with cyanopropyltriethoxysilane (CNPrTEOS) and non-polar methyltrimethoxysilane (MTMOS) to get rid of organophosphate pesticides like diazinon, methidathion, malathion, chlorpyrifos, dicrotophos, and mathamidophos.<sup>180</sup> GC-MS or HPLC are then used to test the pesticides that were extracted from different sources using SiO<sub>2</sub> NPs. Table 9 shows SiO<sub>2</sub> and their composites as adsorbents for the removal of pesticides from the wastewater.

## 7.5 Magnesium oxide

It has been demonstrated that MgO nanoparticles are a promising adsorbent for organic pollutants and hazardous substances.<sup>185,186</sup> Magnesium oxide nanoparticles have a high concentration of low-coordinated sites, controlled textural features, are non-toxic, and have structural flaws, all of which increase their potential for adsorption applications. Furthermore, the adsorption of anionic dyes driven by electrostatic attraction was encouraged by the higher pH (12.4) of the zero-point charge (pH<sub>pzc</sub>) of MgO. Chlorpyrifos (CPF), a persistent pesticide based on organophosphates, was highly adsorbed (3974 mg g<sup>-1</sup>) into the hierarchical porous microspheres of MgO nanosheets that were made by precipitation and calcination.<sup>187</sup> Table 10 shows SiO<sub>2</sub> and their composites as adsorbents for the removal of pesticides from the wastewater.

## 7.6 Other metal oxides

A wide range of distinct metal oxide nanomaterials, such as SnO<sub>2</sub>, Cu<sub>2</sub>O, MoO<sub>3</sub>, MoO<sub>2</sub>, ThO<sub>2</sub>, CeO<sub>2</sub>, etc., have been investigated as adsorbents for wastewater cleanup to remove organic contaminants in addition to iron oxides, titania, zinc oxides, and magnesium oxides. Due to their unique chemical and physical properties, as well as their structural flexibility, manganese oxides have attracted a lot of attention.<sup>192</sup> The MnO<sub>2</sub> nanoparticles' negatively charged surface made it easier for cationic contaminants to stick to them, which was especially true when the pH level was high.<sup>193</sup>

Ni(OH)<sub>2</sub> and NiO are significant transition metal hydroxides and oxides used in a variety of applications, such as energy

storage devices.<sup>194</sup> The geometrical characteristics and chemical makeup of Ni(OH)<sub>2</sub> and NiO regulate their adsorption capacity. When used for effective pesticide removal, the chitosan modified AgO nanoparticles absorbed 99% of the permethrin insecticide from the aqueous solution (0.1 mg L<sup>-1</sup>), 200% more effectively than pure chitosan (49%).<sup>195</sup>

It was shown that the zirconium-based metal-organic frameworks of UiO-67 could adsorptively remove the pesticides glyphosate and glufosinate from an aqueous solution. The presence of Zr-OH groups in large quantities within UiO-67 particles acted as an anchor for the effective adsorption of herbicides such as glyphosate (537 mg g<sup>-1</sup>) and glufosinate (360 mg g<sup>-1</sup>).<sup>196</sup>

## 8. Adsorptive removal versus photocatalytic degradation

In water treatment, two commonly employed techniques for removing organic pollutants are photocatalytic degradation and adsorption. Both methods are efficient and straightforward, but photocatalytic degradation is considered more sustainable than adsorption. While adsorption is a rapid, scalable, and cost-effective technique, it has limitations, as it generates waste after contaminants are absorbed. Additional environmental issues related to adsorption include the disposal of spent adsorbents, potential leaching of pollutants, and challenges in reusing adsorbents for future cycles.<sup>180</sup>

In contrast, photocatalytic degradation converts organic pollutants into less harmful substances or intermediates, eventually yielding mineral end products such as water (H<sub>2</sub>O) and carbon dioxide (CO<sub>2</sub>), thus minimizing waste.<sup>181</sup> Factors that influence photocatalytic efficiency include the photocatalyst's band-gap structure, the light source, and the ability of pollutants to adhere to the photocatalyst's surface. Enhanced adsorption on the photocatalyst surface aids in effective degradation, as it brings the pollutant molecules into close contact with the catalyst, improving photodegradation.

In summary, while adsorption serves as a useful step to facilitate photodegradation, photocatalytic degradation is ultimately a superior approach due to its ability to fully decompose organic pollutants into harmless byproducts. Nonetheless, effective adsorption is essential for achieving optimal photodegradation rates.



## 9. Linking adsorption and photocatalysis: synergistic approaches for pollutant remediation

Adsorption and photocatalysis are two distinct but complementary methods for effectively cleaning up organic pollutants. Surface interactions, like van der Waals forces, hydrogen bonding, or chemical bonding, characterize adsorption as a passive process that immobilizes pollutants in the adsorbent material. It exhibits energy efficiency and functions effectively across diverse environmental conditions without requiring external activation. Photocatalysis is an active process that uses light energy to excite electrons in semiconductors. This creates reactive species like hydroxyl radicals ( $\cdot\text{OH}$ ) and superoxide ions ( $\text{O}_2^{\cdot-}$ ), which help break down pollutants into harmless end products. Photocatalysis necessitates specific conditions, including a suitable light source, optimized material properties, and precise environmental parameters.

The strategic combination of the two methods can enhance remediation efficiency. Adsorption serves as a fundamental capture mechanism, concentrating pollutants on the material's surface. This process removes contaminants from the aqueous phase and facilitates their subsequent degradation. Some materials, like  $\text{TiO}_2$  composites with lots of surfaces or metal oxides that have been doped in, make it easier for reactive species made during photocatalysis to reach pollutants that have stuck to them. This process leads to the total mineralization of pollutants, which addresses challenges like incomplete degradation and secondary contamination. The interaction between adsorption and photocatalysis highlights their potential in creating multifunctional materials for advanced water treatment technologies. This section will examine the intricacies of photocatalytic mechanisms, developments in materials, and their roles in pollutant remediation.

## 10. Summary and future perspectives

Water is essential for the survival of all life forms, yet water pollution has escalated into a critical global issue, with contamination levels rising sharply over time. Numerous remediation techniques have been developed to preserve water quality, each tailored to address specific types of contaminants. Among these, metal oxides and their composites play a significant role as both photocatalytic and adsorptive materials in removing organic pollutants from wastewater. This comprehensive review examines the mechanisms of adsorption and photocatalysis in water treatment, focusing on the various structural, chemical, and surface properties of metal oxide nanomaterials that contribute to their high adsorption efficiency. Different adsorptive pathways—such as chemisorption, physisorption, and charge-driven interactions—demonstrate the versatility of these nanomaterials in capturing organic pollutants.

The application of metal oxide-based nanomaterials and their composites, including those for removing dyes and pesticides from wastewater, is discussed in depth. Materials such as graphene–metal oxide nanocomposites, iron oxides,

magnesium oxides, titanium oxides, zinc oxides, tungsten oxides, and copper oxides have shown remarkable potential in this field. This analysis highlights the advancements, opportunities, and challenges associated with using these materials for water purification.

Adsorption is a widely recognized method for removing various contaminants, especially organic pollutants, by transferring them from an aqueous phase to a solid adsorbent phase. Although effective, it has limitations, including the generation of secondary pollutants. Adsorbents are employed across many industries; however, improvements in recyclability, adsorption efficiency, and eco-friendly decomposition of adsorbed pollutants are needed. Recently, metal oxide nanostructured materials and their composites have gained significant interest as photocatalytic agents, capable of degrading organic pollutants or converting them into environmentally benign products. For example, graphene–metal oxide composites,  $\text{CuO}$ ,  $\text{ZnO}$ ,  $\text{MgO}$ , and  $\text{TiO}_2$  have demonstrated the ability to break down organic contaminants upon exposure to light, and these materials offer the advantage of reusability. However, challenges remain, particularly in scaling up the use of these materials for industrial applications with high efficiency.

Developing these materials sustainably and cost-effectively while achieving optimal performance under solar light exposure has been a persistent obstacle. Engineering the crystal structure and surface properties to enhance solar absorption efficiency is another critical challenge. Moving forward, the goal is to design advanced materials for sustainable water remediation that achieve zero pollutant discharge. This requires scientific innovation to create materials with a high specific surface area, optimal crystalline structures, and compatibility with environmentally friendly, economically viable manufacturing processes. The development of such “smart” materials is crucial for advancing water treatment technology toward sustainable and effective pollution control.

Adsorbent/photocatalyst regeneration is another crucial element that supports the process's sustainability and economic feasibility, prevents hazardous disposal, and preserves the equilibrium between water treatment and secondary waste management. Although it hasn't been thoroughly studied, the management of secondary trash is something that needs to be taken very seriously. Catalysis is one of the numerous uses for secondary waste, or used adsorbent.<sup>197</sup> As a result, the possibility of less pollution during the creation of metal oxide nanoparticles and their use in water treatment, as well as their use for other purposes, may help make the platform greener. It took a lot of work to develop economically viable, quicker, greener, and more effective methods for the removal or degradation of organic contaminants in a sustainable way and for the resurgence of safe and clean water for humans and other living things.

## Data availability

No primary research results, software or code have been included and no new data were generated or analysed as part of this review.



## Author contributions

The listed authors contributed to this work as follows: A. H. K. provided the concepts of the work; A. A., L. A., G. B. S. and H. S. M. A. interpreted the results. A. H. K., A. A. and H. S. M. A. prepared the manuscript; A. H. K. performed the revision before submission. All authors have read and agreed to the published version of the manuscript.

## Conflicts of interest

The authors declare that there are no conflicts of interest.

## Acknowledgements

The author H. S. M. Abd-Rabboh extends his appreciation to the Deanship of Scientific Research at King Khalid University for funding this work through a large Group Project under grant number (RGP.2/122/46).

## References

- 1 G. Devendrapandi, X. Liu, R. Balu, R. Ayyamperumal, M. V. Arasu, M. Lavanya, V. R. M. Reddy, W. K. Kim and P. C. Karthika, *Environ. Res.*, 2024, **118404**.
- 2 M. Wang, B. L. Bodirsky, R. Rijnneveld, F. Beier, M. P. Bak, M. Batool, B. Droppers, A. Popp, M. T. van Vliet and M. Strokal, *Nat. Commun.*, 2024, **15**, 880.
- 3 M. M. Mekonnen, M. M. Kebede, B. W. Demeke, J. A. Carr, A. Chapagain, C. Dalin, P. Debaere, P. D'Odorico, L. Marston, C. Ray and L. Rosa, *Nat. Rev. Earth Environ.*, 2024, **5**, 890–905.
- 4 P. K. Singh, U. Kumar, I. Kumar, A. Dwivedi, P. Singh, S. Mishra, C. S. Seth and R. K. Sharma, *Environ. Sci. Pollut. Res.*, 2024, **31**, 56428–56462.
- 5 M. Rastogi, S. M. Kolur, A. Burud, T. Sadineni, M. Sekhar, R. Kumar and A. Rajput, *J. Geogr. Environ. Earth Sci. Int.*, 2024, **28**, 41–53.
- 6 F. Edition, *WHO Chron.*, 2011, **38**, 104–108.
- 7 R. Kaur, D. Choudhary, S. Bali, S. S. Bandral, V. Singh, M. A. Ahmad, N. Rani, T. G. Singh and B. Chandrasekaran, *Sci. Total Environ.*, 2024, **170113**.
- 8 N. Talat, *Water Conserv. Glob. Clim. Change*, 2021, pp. 47–71.
- 9 L. Wang, C. Shi, L. Pan, X. Zhang and J. J. Zou, *Nanoscale*, 2020, **12**, 4790–4815.
- 10 R. Gusain, K. Gupta, P. Joshi and O. P. Khatri, *Adv. Colloid Interface Sci.*, 2019, **272**, 102009.
- 11 Y. Abubakar, H. Tijjani, C. Egbuna, C. O. Adetunji, S. Kala, T. L. Kryeziu, J. C. Ifemeje and K. C. Patrick-Iwuanyanwu, *Nat. Remedies Pest Dis. Weed Control*, 2020, pp. 29–42.
- 12 A. Shattuck, M. Werner, F. Mempel, Z. Dunivin and R. Galt, *Glob. Environ. Change*, 2023, **81**, 102693.
- 13 M. Tudi, H. Daniel Ruan, L. Wang, J. Lyu, R. Sadler, D. Connell, C. Chu and D. T. Phung, *Int. J. Environ. Res. Public Health*, 2021, **18**, 1112.
- 14 V. M. Pathak, V. K. Verma, B. S. Rawat, B. Kaur, N. Babu, A. Sharma, S. Dewali, M. Yadav, R. Kumari, S. Singh and A. Mohapatra, *Front. Microbiol.*, 2022, **13**, 962619.
- 15 K. K. Gautam and V. K. Tyagi, *J. Oleo Sci.*, 2006, **55**, 155–166.
- 16 S. G. Parte, A. D. Mohekar and A. S. Kharat, *Afr. J. Microbiol. Res.*, 2017, **11**, 992–1012.
- 17 M. L. Ortiz-Hernández, E. Sánchez-Salinas, E. Dantán-González and M. L. Castrejón-Godínez, *Biodegrad.: Life Sci.*, 2013, **10**, 251–287.
- 18 A. D. Kumar and N. Reddy, *Adverse Effects of Pesticides*, 2024.
- 19 R. Kaur, D. Choudhary, S. Bali, S. S. Bandral, V. Singh, M. A. Ahmad, N. Rani, T. G. Singh and B. Chandrasekaran, *Sci. Total Environ.*, 2024, **170113**.
- 20 N. L. Mdeni, A. O. Adeniji, A. I. Okoh and O. O. Okoh, *Molecules*, 2022, **27**, 618.
- 21 P. G. Bertrand, *Pesticides*, 2019, 1–14.
- 22 P. M. Njogu, *Assessment Pollution Prediction Environ. Risks*, 2014.
- 23 O. G. Okon and U. E. Antia, *One Health Implications Agrochemicals*, 2023, pp. 441–460.
- 24 M. Shahid and M. S. Khan, *Pestic. Biochem. Physiol.*, 2022, **188**, 105272.
- 25 S. Antunes-Kenyon and G. Kennedy, *Massachusetts Dep. Agric. Resour.*, 2004.
- 26 D. K. Hazra and A. Purkait, *J. Pharmacogn. Phytochem.*, 2019, **8**, 686–693.
- 27 N. Chaudhary, K. K. Choudhary, S. Agrawal and M. Agrawal, *Pestic. Crop Prod.*, 2020, 159–180.
- 28 W. Draber, K. Tietjen, J. F. Kluth and A. Trebst, *Angew. Chem., Int. Ed.*, 1991, **30**, 1621–1633.
- 29 J. A. Martinez, Natural fungicides obtained from plants, *Fungicides for Plant and Animal Diseases*, ed. D. Dhanasekaran, InTech, 2012, vol. 10, p. 26336, ISBN: 978-953-307-804-5.
- 30 K. S. Rajmohan, R. Chandrasekaran and S. Varjani, *Indian J. Microbiol.*, 2020, **60**, 125–138.
- 31 M. L. Chen, X. W. Yao, Z. H. Diao, J. C. Jin, W. Qian, Y. Q. Yi, X. Chen and L. J. Kong, *Sep. Purif. Technol.*, 2023, **327**, 125013.
- 32 R. Gao, S. H. Gao, J. Li, Y. Su, F. Huang, B. Liang, L. Fan, J. Guo and A. Wang, *Engineering*, 2024, DOI: [10.1016/j.eng.2024.08.022](https://doi.org/10.1016/j.eng.2024.08.022).
- 33 N. N. Roslan, H. L. H. Lau, N. A. A. Suhaimi, N. N. M. Shahri, S. B. Verinda, M. Nur, J. W. Lim and A. Usman, *Catalysts*, 2024, **14**, 189.
- 34 M. H. Shahverdian, F. Delfani, M. Z. Pedram, M. Hosseini, A. Sohani, H. Fazeli and H. Sayyaadi, *Sustainable Technol. Remediation Pollut.*, 2024, pp. 13–28.
- 35 O. A. Abiodun and O. O. Ayeleru, *Smart Nanomater. Environ. Appl.*, 2025, pp. 487–525.
- 36 R. Meena, M. M. Abdullah, V. Vasanthakumar, D. Ravichandran and S. Murugesan, *Ionics*, 2024, **30**, 5639–5650.
- 37 T. H. H. Al-Aqbi, T. Rafique, I. Mazahirul, S. M. H. Gardazi, W. Ahmad, A. Gupta, R. F. Alshehri and M. M. Ali, *Nanomater. Environ. Remediat.*, 2024.



38 Z. H. Diao and W. Chu, *Sci. Total Environ.*, 2021, **754**, 142155.

39 Y. Khan, H. Sadia, S. Z. Ali Shah, M. N. Khan, A. A. Shah, N. Ullah, M. F. Ullah, H. Bibi, O. T. Bafakeeh, N. B. Khedher and S. M. Eldin, *Catalysts*, 2022, **12**, 1386.

40 J. C. Védrine, *ChemSusChem*, 2019, **12**, 577–588.

41 L. Wang, C. Shi, L. Pan, X. Zhang and J. J. Zou, *Nanoscale*, 2020, **12**, 4790–4815.

42 K. V. Kumar, S. Gadielli, B. Wood, K. A. Ramisetty, A. A. Stewart, C. A. Howard, D. J. Brett and F. Rodriguez-Reinoso, *J. Mater. Chem. A*, 2019, **7**, 10104–10137.

43 M. M. Sabzehei, S. Mahnaee, M. Ghaedi, H. Heidari and V. A. Roy, *Mater. Adv.*, 2021, **2**, 598–627.

44 R. Gusain, K. Gupta, P. Joshi and O. P. Khatri, *Adv. Colloid Interface Sci.*, 2019, **272**, 102009.

45 S. Gautam, H. Agrawal, M. Thakur, A. Akbari, H. Sharda, R. Kaur and M. Amini, *J. Environ. Chem. Eng.*, 2020, **8**, 103726.

46 M. A. Gatou, A. Syrrakou, N. Lagopati and E. A. Pavlatou, *Reactions*, 2024, **5**, 135–194.

47 K. Kaur, R. Badru, P. P. Singh and S. Kaushal, *J. Environ. Chem. Eng.*, 2020, **8**, 103666.

48 A. Saravanan, P. S. Kumar, S. Jeevanantham, S. Karishma, B. Tajsabreen, P. R. Yaashikaa and B. Reshma, *Chemosphere*, 2021, **280**, 130595.

49 N. K. Elumalai, C. Vijila, R. Jose, A. Uddin and S. Ramakrishna, *Mater. Renewable Sustainable Energy*, 2015, **4**, 1–25.

50 R. B. Marcelino and C. C. Amorim, *Environ. Sci. Pollut. Res.*, 2019, **26**, 4155–4170.

51 A. Venkateshaiah, M. Černík and V. V. Padil, *Nanotechnol. Environ. Remediat.*, 2022, pp. 183–213.

52 P. Joshi, K. Gupta, R. Gusain and O. P. Khatri, *Metal Oxide Nanocomposites: Synthesis and Applications*, 2020, pp. 361–397.

53 R. Gusain, K. Gupta, P. Joshi and O. P. Khatri, *Adv. Colloid Interface Sci.*, 2019, **272**, 102009.

54 I. Ali, M. Suhail, E. C. López, R. A. Khattab and H. M. Albishri, *Arabian J. Geosci.*, 2022, **15**, 521.

55 M. A. Bhatti, A. A. Shah, K. F. Almani, A. Tahira, S. E. Chalangar, A. Chandio, O. Nur, M. Willander and Z. H. Ibupoto, *Ceram. Int.*, 2019, **45**, 23289–23297.

56 H. Chawla, S. Garg, J. Rohilla, Á. Szamosvölgyi, A. Efremova, I. Szenti, P. P. Ingole, A. Sápi, Z. Kónya and A. Chandra, *J. Cleaner Prod.*, 2022, **367**, 132923.

57 B. Karthikeyan, G. Gnanakumar and A. T. Alphonsa, *Nano Metal Oxides*, 2023.

58 *Handbook of Green and Sustainable Nanotechnology: Fundamentals, Developments and Applications*, ed. U. Shanker, C. M. Hussain and M. Rani, Springer Nature, 2023.

59 I. Abdelfattah and A. M. El-Shamy, *Sci. Rep.*, 2024, **14**, 27175.

60 A. A. M. Raub, R. Bahru, M. A. Mohamed, R. Latif, M. A. S. M. Haniff, K. Simarani and J. Yunas, *Nanotechnology*, 2024, **35**, 242004.

61 M. Ortiz-Martínez, J. A. Molina González, G. Ramírez García, A. Luna Bugallo, M. A. Justo Guerrero and E. C. Strupiechonski, *Environ. Toxicol. Chem.*, 2024, **43**, 1468–1484.

62 I. Arora, H. Chawla, A. Chandra, S. Sagadevan and S. Garg, *Inorg. Chem. Commun.*, 2022, **143**, 109700.

63 M. M. Mahlambi, C. J. Ngila and B. B. Mamba, *J. Nanomater.*, 2015, **2015**, 790173.

64 K. Nagaveni, M. S. Hegde, N. Ravishankar, G. N. Subbanna and G. Madras, *Langmuir*, 2004, **20**, 2900–2907.

65 A. T. Kuvarega and B. B. Mamba, *Crit. Rev. Solid State Mater. Sci.*, 2017, **42**, 295–346.

66 J. F. Budarz, E. M. Cooper, C. Gardner, E. Hodzic, P. L. Ferguson, C. K. Gunsch and M. R. Wiesner, *J. Hazard. Mater.*, 2019, **372**, 61–68.

67 R. Goswami, B. Kamal and A. Mishra, *Pestic. Bioremediation*, 2022, pp. 281–309.

68 S. N. Hoseini, A. K. Pirzaman, M. A. Aroon and A. E. Pirbazari, *J. Water Process Eng.*, 2017, **17**, 124–134.

69 M. Mehdipour, A. E. Pirbazari and G. Khayati, *Desalin. Water Treat.*, 2019, **155**, 329–340.

70 T. Kaur, A. Sraw, R. K. Wanchoo and A. P. Toor, *Sol. Energy*, 2018, **162**, 45–56.

71 R. de Oliveira and A. C. Sant'Ana, *Chemosphere*, 2023, **338**, 139490.

72 R. Fiorenza, A. Di Mauro, M. Cantarella, C. Iaria, E. M. Scalisi, M. V. Brundo, A. Gulino, L. Spitaleri, G. Nicotra, S. Dattilo and S. C. Carroccio, *Chem. Eng. J.*, 2020, **379**, 122309.

73 M. A. Rauf, M. A. Meetani and S. Hisaindee, *Desalination*, 2011, **276**, 13–27.

74 M. Janus, *Titanium Dioxide*, BoD – Books on Demand, 2017, ch. 2, 9789535134138.

75 D. Madan, K. P. Misra, S. Chattopadhyay and N. Halder, *Ceram. Sci. Eng.*, 2022, pp. 215–234.

76 K. Singh, S. Harish, J. Archana, M. Navaneethan, M. Shimomura and Y. Hayakawa, *Appl. Surf. Sci.*, 2019, **489**, 883–892.

77 M. Sattari, M. Farhadian, A. R. S. Nazar and M. Moghadam, *J. Photochem. Photobiol. A*, 2022, **431**, 114065.

78 S. R. Mirmasoomi, M. M. Ghazi and M. Galedari, *Sep. Purif. Technol.*, 2017, **175**, 418–427.

79 S. Nasseri, M. O. Borna, A. Esrafil, R. R. Kalantary, B. Kakavandi, M. Sillanpää and A. Asadi, *Appl. Phys. A*, 2018, **124**, 329–340.

80 A. H. C. Khavar, G. Moussavi, A. R. Mahjoub, M. Satari and P. Abdolmaleki, *Chem. Eng. J.*, 2018, **345**, 300–311.

81 G. Li, B. Wang, W. Q. Xu, Y. Han and Q. Sun, *Dyes Pigm.*, 2018, **155**, 265–275.

82 S. Raha and M. Ahmaruzzaman, *Nanoscale Adv.*, 2022, **4**, 1868–1925.

83 S. Maiti, S. Pal and K. K. Chattopadhyay, *CrystEngComm*, 2015, **17**, 9264–9295.

84 C. Hariharan, *Appl. Catal. A*, 2006, **304**, 55–61.

85 N. Daneshvar, D. Salari and A. R. Khataee, *J. Photochem. Photobiol. A*, 2004, **162**, 317–322.



86 N. Daneshvar, S. Aber, M. S. Dorraji, A. R. Khataee and M. H. Rasoulifard, *Sep. Purif. Technol.*, 2007, **58**, 91–98.

87 S. Navarro, J. Fenoll, N. Vela, E. Ruiz and G. Navarro, *J. Hazard. Mater.*, 2009, **172**, 1303–1310.

88 E. K. Kirupa Vasam Jino, *Adv. Environ. Technol.*, 2023, **9**, 124–137.

89 F. H. Abdullah, N. A. Bakar and M. A. Bakar, *J. Hazard. Mater.*, 2022, **424**, 127416.

90 N. Daneshvar, S. Aber, M. S. Dorraji, A. R. Khataee and M. H. Rasoulifard, *Sep. Purif. Technol.*, 2007, **58**, 91–98.

91 T. Iqbal, M. Afzal, B. A. Al-Asbahi, S. Afsheen, I. Maryam, A. Mushtaq, S. Kausar and A. Ashraf, *Mater. Sci. Semicond. Process.*, 2024, **173**, 108152.

92 S. M. Hosseini, I. A. Sarsari, P. Kameli and H. Salamat, *J. Alloys Compd.*, 2015, **640**, 408–415.

93 N. Güy, S. Çakar and M. Özcar, *J. Colloid Interface Sci.*, 2016, **466**, 128–137.

94 S. Bhatia, N. Verma and R. K. Bedi, *Opt. Mater.*, 2016, **62**, 392–398.

95 A. Nezamzadeh-Ejhieh and F. Khodabakhshi-Chermahini, *J. Ind. Eng. Chem.*, 2014, **20**, 695–704.

96 A. A. Khodja, T. Sehili, J. F. Pilichowski and P. Boule, *J. Photochem. Photobiol. A*, 2001, **141**, 231–239.

97 N. Daneshvar, S. Aber, M. S. Dorraji, A. R. Khataee and M. H. Rasoulifard, *Sep. Purif. Technol.*, 2007, **58**, 91–98.

98 S. Navarro, J. Fenoll, N. Vela, E. Ruiz and G. Navarro, *J. Hazard. Mater.*, 2009, **172**, 1303–1310.

99 W. Wu, C. Jiang and V. A. Roy, *Nanoscale*, 2015, **7**, 38–58.

100 M. Mishra and D. M. Chun, *Appl. Catal. A*, 2015, **498**, 126–141.

101 C. T. Wang, *J. Non-Cryst. Solids*, 2007, **353**, 1126–1133.

102 P. Hao, G. Wang, J. Wen, X. Li, Y. Suo, H. Zhan, S. Bi and W. Liu, *J. Environ. Chem. Eng.*, 2022, **10**, 107728.

103 N. S. M. Shahrodin, J. Jaafar, A. R. Rahmat, N. Yusof, M. H. Dzarfan Othman and M. A. Rahman, *Micro Nano Syst.*, 2020, **12**, 4–22.

104 N. Arif, M. N. Zafar, M. Batool, M. Humayun, M. A. Iqbal, M. Younis, L. Li, K. Li and Y. J. Zeng, *J. Mater. Chem. C*, 2024, **12**, 12653–12691.

105 V. Selvaraj, T. S. Karthika, C. Mansiya and M. Alagar, *J. Mol. Struct.*, 2021, **1224**, 129195.

106 E. Akhayere, D. Kavaz and A. Vaseashta, *Appl. Sci.*, 2022, **12**, 9279.

107 G. Bapat, C. Labade, A. Chaudhari and S. Zinjarde, *Adv. Colloid Interface Sci.*, 2016, **237**, 1–14.

108 X. P. Kong, B. H. Zhang and J. Wang, *J. Agric. Food Chem.*, 2021, **69**, 6735–6754.

109 D. Rawtani, N. Khatri, S. Tyagi and G. Pandey, *J. Environ. Manage.*, 2018, **206**, 749–762.

110 M. J. Lerma-García, E. F. Simó-Alfonso, M. Zougagh and Á. Ríos, *Talanta*, 2013, **105**, 372–378.

111 W. A. W. Ibrahim, W. N. W. Ismail and M. M. Sanagi, *J. Teknol.*, 2013, **62**, 3.

112 N. Sadegh, A. Asfaram, H. Javadian, H. Haddadi and E. Sharifpour, *J. Chromatogr. B*, 2021, **1171**, 122640.

113 S. B. Al Massati, Synthesis and characterization of molecularly imprinted polymers for the selective extraction of organophosphorus pesticides from vegetable oils, *Doctoral dissertation*, Université Pierre et Marie Curie-Paris VI, 2017.

114 N. Farooq, Z. ur Rehman, M. I. Khan, W. Iman, I. Kanwal, S. Khan, A. Shanableh, S. Manzoor and R. Luque, *Inorg. Chem. Commun.*, 2024, 113086.

115 R. Gusain, K. Gupta, P. Joshi and O. P. Khatri, *Adv. Colloid Interface Sci.*, 2019, **272**, 102009.

116 S. Tsunekawa, J. T. Wang and Y. Kawazoe, *J. Alloys Compd.*, 2006, **408**, 1145–1148.

117 A. Salerno, I. Pitault, T. Devers, J. Pelletier and S. Briançon, *Environ. Toxicol. Pharmacol.*, 2017, **53**, 18–28.

118 R. Fiorenza, S. A. Balsamo, L. D'Urso, S. Sciré, M. V. Brundo, R. Pecoraro, E. M. Scalisi, V. Privitera and G. Impellizzeri, *Catalysts*, 2020, **10**, 446.

119 P. Janos, P. Kuran, M. Kormunda, V. Stengl, T. M. Grygar, M. Dosek, M. Stastny, J. Ederer, V. Pilarova and L. Vrtoch, *J. Rare Earths*, 2014, **32**, 360–370.

120 P. Janoš, P. Kuráň, V. Pilařová, J. Trögl, M. Šťastný, O. Pelant, J. Henych, S. Bakardjieva, O. Životský, M. Kormunda and K. Mazanec, *Chem. Eng. J.*, 2015, **262**, 747–755.

121 M. K. Diallo, *SSRN Electron. J.*, 2022, 4441684.

122 D. Xiong, C. Fei, L. Qizeng and D. Ping, *Catal. Today*, 2014, **226**, 171–178.

123 C. M. Magdalane, K. Kaviyarasu, J. J. Vijaya, B. Siddhardha, B. Jeyaraj, J. Kennedy and M. Maaza, *J. Alloys Compd.*, 2017, **727**, 1324–1337.

124 T. K. Wong, S. Zhuk, S. Masudy-Panah and G. K. Dalapati, *Materials*, 2016, **9**, 271.

125 V. Molahalli, A. Sharma, K. Bijapur, G. Soman, A. Shetty, B. Sirichandana, B. M. Patel, N. Chattham and G. Hegde, *ACS Nano*, 2024, **18**, 33.

126 P. Raizada, A. Sudhaik, S. Patial, V. Hasija, A. A. P. Khan, P. Singh, S. Gautam, M. Kaur and V. H. Nguyen, *Arabian J. Chem.*, 2020, **13**, 8424–8457.

127 D. Malwal and P. Gopinath, *Catal. Sci. Technol.*, 2016, **6**, 4458–4472.

128 A. A. Umar and M. Oyama, *Cryst. Growth Des.*, 2007, **7**, 2404–2409.

129 S. Jung and K. Yong, *Chem. Commun.*, 2011, **47**, 2643–2645.

130 A. Chawla, A. Sudhaik, P. Raizada, A. A. P. Khan, A. Singh, Q. Van Le, T. Ahamad, S. M. Alshehri, A. M. Asiri and P. Singh, *J. Ind. Eng. Chem.*, 2022, **116**, 515–542.

131 N. Bayal and P. Jeevanandam, *Mater. Res. Bull.*, 2013, **48**, 3790–3799.

132 S. Bai, K. Zhang, J. Sun, R. Luo, D. Li and A. Chen, *CrystEngComm*, 2014, **16**, 3289–3295.

133 S. Bai, H. Liu, J. Sun, Y. Tian, S. Chen, J. Song, R. Luo, D. Li, A. Chen and C. C. Liu, *Appl. Surf. Sci.*, 2015, **338**, 61–68.

134 M. Long, W. Cai, J. Cai, B. Zhou, X. Chai and Y. Wu, *J. Phys. Chem. B*, 2006, **110**, 20211–20216.

135 H. Chawla, S. Garg, S. Upadhyay, J. Rohilla, Á. Szamosvölgyi, A. Sapi, P. P. Ingole, S. Sagadevan, Z. Konya and A. Chandra, *Chemosphere*, 2022, **297**, 134122.

136 H. Chawla, A. Chandra, P. P. Ingole and S. Garg, *J. Ind. Eng. Chem.*, 2021, **95**, 1–15.



137 W. Raza, M. M. Haque, M. Muneer, T. Harada and M. Matsumura, *J. Alloys Compd.*, 2015, **648**, 641–650.

138 X. W. Yao, X. Chen, M. L. Chen, N. J. Feng, L. Y. Tong, Y. Q. Yi, W. Qian and Z. H. Diao, *Process Saf. Environ. Prot.*, 2024, **186**, 808–818.

139 R. Natarajan, K. Saikia, S. K. Ponnusamy, A. K. Rathankumar, D. S. Rajendran, S. Venkataraman, D. B. Tannani, V. Arvind, T. Somanna, K. Banerjee and N. Mohideen, *Chemosphere*, 2022, **287**, 131958.

140 M. H. Dehghani, S. Ahmadi, S. Ghosh, M. S. Khan, A. Othmani, W. A. Khanday, Ö. Gökkuş, C. Osagie, M. Ahmaruzzaman, S. R. Mishra and E. C. Lima, *Appl. Surf. Sci. Adv.*, 2024, **19**, 100558.

141 H. H. Shanaah, E. F. Alzaimoor, S. Rashdan, A. A. Abdalhafith and A. H. Kamel, *Sustainability*, 2023, **15**, 7336.

142 L. W. Bruch, M. W. Cole and E. Zaremba, *Phys. Adsorpt. Forces Phenom.*, 2007.

143 D. C. Wang, Y. H. Li, D. Li, Y. Z. Xia and J. P. Zhang, *Renewable Sustainable Energy Rev.*, 2010, **14**, 344–353.

144 M. Králik, *Chem. Pap.*, 2014, **68**, 1625–1638.

145 A. Clark, *Chemisorptive Bond Basic Concepts*, 2012, vol. 32.

146 C. C. Okpala, *Int. J. Eng. Res. Dev.*, 2013, **8**, 17–23.

147 M. H. Dehghani, S. Ahmadi, S. Ghosh, M. S. Khan, A. Othmani, W. A. Khanday, Ö. Gökkuş, C. Osagie, M. Ahmaruzzaman, S. R. Mishra and E. C. Lima, *Appl. Surf. Sci. Adv.*, 2024, **19**, 100558.

148 R. M. Cornell and U. Schwertmann, *Iron Oxides Struct. Prop. React. Uses*, 2003, vol. 664.

149 M. E. McHenry and D. E. Laughlin, *Acta Mater.*, 2000, **48**, 223–238.

150 A. M. Gutierrez, T. D. Dziubla and J. Z. Hilt, *Rev. Environ. Health*, 2017, **32**, 111–117.

151 F. X. Dong, L. Yan, X. H. Zhou, S. T. Huang, J. Y. Liang, W. X. Zhang, Z. W. Guo, P. R. Guo, W. Qian, L. J. Kong and W. Chu, *J. Hazard. Mater.*, 2021, **416**, 125930.

152 R. Gusain, K. Gupta, P. Joshi and O. P. Khatri, *Adv. Colloid Interface Sci.*, 2019, **272**, 102009.

153 P. Kajitvichyanukul, V. H. Nguyen, T. Boonupara, L. A. P. Thi, A. Watcharenwong, S. Sumitsawan and P. Udomkun, *Environ. Res.*, 2022, **212**, 113336.

154 Y. Wang, R. Cheng, Z. Wen and L. Zhao, *Chem. Eng. J.*, 2012, **181**, 823–827.

155 F. Liu, H. Tian and J. He, *J. Colloid Interface Sci.*, 2014, **419**, 68–72.

156 A. Ouali, L. S. Belaroui, A. Bengueddach, A. L. Galindo and A. Peña, *Appl. Clay Sci.*, 2015, **115**, 67–75.

157 S. Fiorilli, L. Rivoira, G. Cali, M. Appendini, M. C. Bruzzoniti, M. Coisson and B. Onida, *Appl. Surf. Sci.*, 2017, **411**, 457–465.

158 C. Fan, Y. Liang, H. Dong, G. Ding, W. Zhang, G. Tang, J. Yang, D. Kong, D. Wang and Y. Cao, *Anal. Chim. Acta*, 2017, **975**, 20–29.

159 F. Liu, H. Tian and J. He, *J. Colloid Interface Sci.*, 2014, **419**, 68–72.

160 W. Liu, X. Jiang and X. Chen, *Appl. Surf. Sci.*, 2014, **320**, 764–771.

161 L. Fang, J. Hou, C. Xu, Y. Wang, J. Li, F. Xiao and D. Wang, *Appl. Surf. Sci.*, 2018, **442**, 45–53.

162 A. Markowska-Szczupak, M. Endo-Kimura, O. Paszkiewicz and E. Kowalska, *Nanomaterials*, 2020, **10**, 2065.

163 U. Qumar, J. Z. Hassan, R. A. Bhatti, A. Raza, G. Nazir, W. Nabgan and M. Ikram, *J. Mater. Sci. Technol.*, 2022, **131**, 122–166.

164 J. Zhang, G. Xiao, F. X. Xiao and B. Liu, *Mater. Chem. Front.*, 2017, **1**, 231–250.

165 M. Hadei, A. Mesdaghinia, R. Nabizadeh, A. H. Mahvi, S. Rabbani and K. Naddafi, *Environ. Sci. Pollut. Res.*, 2021, **28**, 13055–13071.

166 M. Gholami, Z. Mosakhani, A. Barazandeh and H. Karyab, *J. Environ. Health Sci. Eng.*, 2023, **21**, 35–45.

167 T. Benhalima, M. Mokhtari and H. Ferfera-Harrar, *J. Water Process Eng.*, 2024, **57**, 104670.

168 A. Barazandeh, H. A. Jamali and H. Karyab, *Korean J. Chem. Eng.*, 2021, **38**, 2436–2445.

169 H. Su, Y. Lin, Z. Wang, Y. L. E. Wong, X. Chen and T. W. D. Chan, *J. Chromatogr. A*, 2016, **1466**, 21–28.

170 Y. Kaur, Y. Bhatia, S. Chaudhary and G. R. Chaudhary, *J. Mol. Liq.*, 2017, **234**, 94–103.

171 S. M. Dehaghi, B. Rahmanifar, A. M. Moradi and P. A. Azar, *J. Saudi Chem. Soc.*, 2014, **18**(4), 348–355.

172 A. U. Haq, M. Saeed, M. Muneer, M. A. Jamal, T. Maqbool and T. Tahir, *Sci. Rep.*, 2022, **12**, 5840.

173 S. M. Dehaghi, B. Rahmanifar, A. M. Moradi and P. A. Azar, *J. Saudi Chem. Soc.*, 2014, **18**(4), 348–355.

174 Z. Samuel, M. O. Ojemaye, O. O. Okoh and A. I. Okoh, *Mater. Today Commun.*, 2023, **34**, 105435.

175 K. Sen and N. K. Mondal, *J. Ind. Eng. Chem.*, 2024, **136**, 150–166.

176 L. K. Harada, M. Guilger-Casagrande, T. Germano-Costa, N. Bilesky-José, L. F. Fraceto and R. Lima, *Silicon Adv. Sustainable Agric. Hum. Health*, 2024, pp. 191–208.

177 S. H. Wu, C. Y. Mou and H. P. Lin, *Chem. Soc. Rev.*, 2013, **42**(9), 3862–3875.

178 J. Tejedor, V. H. Guerrero, K. Vizuete and A. Debut, *J. Phys.: Conf. Ser.*, 2022, **2238**, 012005.

179 V. Bueno, *Synthesis, Characterization and Application of Pesticide-Encapsulated Silica Nanoparticles in Agriculture*, McGill University, Canada, 2021.

180 N. Muhamad, W. A. W. Ibrahim and M. M. Sanagi, *J. Teknol.*, 2014, **71**(5), 57–62.

181 F. Malhat, O. I. Abdallah, M. Hussien, A. M. Youssef, F. M. Alminderej and S. M. Saleh, *Coatings*, 2023, **13**(7), 1286.

182 S. N. Ul Ain, M. S. Khan, N. Riaz, A. Khan, A. Sarwar, A. Khalid, A. Jan, Q. Mahmood and A. Al-Harrasi, *ACS Omega*, 2024, **9**(12), 13803–13817.

183 G. Wu, C. Zhang, C. Liu, X. Li, Y. Cai, M. Wang, D. Chu, L. Liu, T. Meng and Z. Chen, *J. Hazard. Mater.*, 2023, **457**, 131788.

184 A. Bekhoukh, M. Kiari, I. Moulefera, L. Sabantina and A. Benyoucef, *Polymers*, 2023, **15**(9), 2032.

185 M. Nagpal and R. Kakkar, *Sep. Purif. Technol.*, 2019, **211**, 522–539.



186 A. Fouda, S. E. D. Hassan, E. Saied and M. F. Hamza, *J. Environ. Chem. Eng.*, 2021, **9**(4), 105346.

187 L. Sharma and R. Kakkar, *ACS Appl. Mater. Interfaces*, 2017, **9**(44), 38629–38642.

188 A. Kar, S. Deole, B. G. Gadratagi, N. Patil, G. Guru-Pirasanna-Pandi, B. Mahapatra and T. Adak, *Environ. Sci. Pollut. Res.*, 2023, **30**(45), 101467–101482.

189 X. Chen, X. W. Yao, Y. Diao, H. Liu, M. L. Chen, N. J. Feng, W. Qian, X. H. Zhou, P. R. Guo, L. J. Kong and Z. H. Diao, *Sep. Purif. Technol.*, 2024, **336**, 126213.

190 L. Y. George, L. Ma, W. Zhang and G. Yao, *Environ. Sci. Eur.*, 2023, **35**(1), 21.

191 L. Sharma and R. Kakkar, *J. Environ. Chem. Eng.*, 2018, **6**(6), 6891–6903.

192 S. Chaudhary, Y. Kaur, A. Umar and G. R. Chaudhary, *J. Mol. Liq.*, 2016, **224**, 1294–1304.

193 A. K. Sharma, R. K. Tiwari and M. S. Gaur, *Arabian J. Chem.*, 2016, **9**, 1755–1764.

194 D. U. Lee, J. Fu, M. G. Park, H. Liu, A. Ghorbani Kashkooli and Z. Chen, *Nano Lett.*, 2016, **16**(3), 1794–1802.

195 M. V. Bagal and S. Raut-Jadhav, in *Handbook of Nanomaterials for Wastewater Treatment*, Elsevier, 2021, pp. 957–1007.

196 F. Fang, Q. Lv, P. Li, Y. Tao, Y. Zhang, Y. Zhou, X. Li and J. Li, *J. Environ. Chem. Eng.*, 2022, **10**(3), 107824.

197 T. Velempini, M. E. H. Ahamed and K. Pillay, *Results Chem.*, 2023, **5**, 100901.

